QATAR UNIVERSITY

COLLEGE OF ENGINEERING

HARVESTING OF *CHLORELLA* SP. MICROALGAE BY DIELECTROPHORETIC FORCE USING TITANIUM DIOXIDE (TiO_2) INSULATED ELECTRODES

BY

AFNAN ABDIRASHID MUSSA

A Thesis Submitted to

the College of Engineering

in Partial Fulfillment of the Requirements for the Degree of

Master of Science in Environmental Engineering

January 2022

COMMITTEE PAGE

The members of the Committee approve the Thesis of
Afnan Abdirashid Mussa defended on 24/11/2021.

Prof. Alaa H. Al Hawari
Thesis/Dissertation Supervisor

Prof. Abdelbaki Benamor
Internal Examiner

Approved:

Khalid Kamal Naji, Dean, College of Engineering

ABSTRACT

MUSSA, AFNAN, A., Masters: January: 2022, Masters of Science in Environmental Engineering

Title: Harvesting of *Chlorella* sp. Microalgae by Dielectrophoretic Force Using Titanium Dioxide (TiO_2) Insulated Electrodes

Supervisor of Thesis: Alaa, H., Al Hawari.

The harvesting of microalgae using conventional technologies suffers from biomass contamination, high energy consumption and long processing time. In this study, titanium dioxide (TiO_2) insulated stainless steel electrodes were used for the harvesting of *Chlorella* sp. microalgae by dielectrophoretic force. The new electrode configuration is expected to achieve high harvesting efficiency with zero contamination for the harvested biomass. The effect of various experimental parameters on the harvesting efficiency were evaluated using a bench scale setup. This includes settling time, applied voltage, interelectrode distance, application of pulsed electric field, and applied current frequency. The maximum harvesting efficiency of 76.6% was obtained at 4 mm interelectrode distance, 200 V applied voltage, 250 kHz frequency, and application of pulsed electric field for 30 minutes. Under these conditions, the energy consumption was 7.76 kWh/kg. The most significant impact of using the new electrode configuration is achieving high harvesting efficiency with no contamination for the biomass.

DEDICATION

This thesis is dedicated to my parents, my sister, and my brothers for the continuous support, and to my supervisor for assisting and guiding me. This work is also dedicated to my friends for the constant encouragement and support.

ACKNOWLEDGMENTS

I would like to express my gratitude to my supervisor Dr. Alaa Al Hawari, who gave me the opportunity to work on such an interesting project, and who without his continuous support and guidance the completion of my thesis would not have been possible. I would like to extend my sincere thanks to Eng. Mhd Hafiz and Eng. Ahmed Toki for assisting me through the experimental work. Finally, I must express my deepest gratitude to my family members for their continuous prayers for me, and my friends in Qatar who have been my second family during the challenging journey of graduate studies.

TABLE OF CONTENTS

LIST OF TABLES

LIST OF FIGURES

Chapter 1: Introduction

1.1 Research Overview

Microalgae are unicellular and multicellular microorganisms that include prokaryotic microalgae (i.e., cyanobacteria), eukaryotic microalgae such as green algae, red algae, and diatoms (Brennan & Owende, 2010). With the presence of CO_2, air, and nutrients (Dineshbabu et al., 2019), microalgae have the ability to convert 9-10% of solar energy into organic biomass with a theoretical yield of approximately 77 $g.biomass^{-1}.m^{-2}.day^{-1}$ (Melis, 2009). The importance of microalgae is due to their short production turnover (less than 15 days) (Brennan & Owende, 2010), simple growth requirements in arable land and freshwater (G. Singh & Patidar, 2018), highest photosynthetic productivity on earth which is more than 50%, potential for year round production (J. Singh & Gu, 2010), and their richness with valuable products such as proteins, lipids, and carbohydrates (Dineshbabu et al., 2019; Gouveia et al., 2017). Furthermore, the economic value of microalgal biomass represented in its world market of 6×10^9 U.S$/year, with around 7.5×10^6 ton/year of macroalgae harvested, and 5,000 tons/year of dry biomass matter produced (Pulz & Gross, 2004). Microalgae is rich with valuable components which can be utilized directly or indirectly in various applications such as biofuels, health supplements and pharmaceuticals, and cosmetics. Furthermore, the interest in utilizing microalgae in wastewater treatment and atmospheric CO_2 mitigation have been increasing (Khan et al., 2018). The major components of microalgae are proteins counting for more than half (i.e., 40 - 65%) of its biomass in some species (Vaz et al., 2016). This protein is important as nutritious component for human body, due to the presence of all the essential amino acids required for human growth. It is reported that the protein content found in some microalgae species are

higher than the protein found in protein rich food such as eggs and soybean (i.e., 610 g/Kg of protein in microalgae and 370 g/Kg protein in soybean) (Buono et al., 2014). Another valuable microalga component is lipids which can be accumulated in large quantities under stress environments (Adarme-Vega et al., 2012). For example, some microalgae species contain omega-3 fatty acids accounting for approx. 30-40% of their total fatty acid components. It is reported that the consumption of omega-3 fatty acids is important to cure cardiovascular and neurodegenerative diseases, and to develop brain function and nervous system especially in children (Wysoczański et al., 2016). Additional nutritious components in microalgae are vitamins such as Vitamin A, B1, B2, B6, B12, C, E, K, niacin, nicotinate, biotin, and folic acid. In addition to minerals which counts for 2.2-4.8% of total dry biomass weight such as Ca, P, Mg, K, Na, Zn, Fe, Cu, and S (Fox & Zimba, 2018). Biofuel from microalgae is considered as a promising renewable and sustainable energy source, and a cleaner alternative for fossil fuels. Microalgal cells accumulate around 50-70% of lipids and reach up to 80% in some species (Mata et al., 2010), hence produce 58,700 L/hac of oil (Medipally et al., 2015). One of the most common biofuels are bioethanol which is produced by the conversion of carbohydrates such as glycogen, starch, agar, and cellulose, to fermentable sugars. Production of bioethanol from microalgae is significant for the improvement of sustainable biofuels due to its ease of production and its advantages over other biofuels (Goldemberg, 2007). Another important biofuel is biodiesel which can be produced from most of the microalgae species. Although of the importance of biofuels from microalgae, however the large-scale production and commercialization is limited, and it is considered economically infeasible due to high operational and maintenance costs mainly due to harvesting and conversion processes.

The production process of algal byproducts includes three main steps; cultivation of microalgae, harvesting of microalgae and the extraction of bioproduct from the sample (Khoo et al., 2020), as shown in Figure 1. After the cultivation of microalgae species, the volume of the suspension must be reduced, and microalgae must be harvested for reusing in further applications. Harvesting of microalgae is the process of concentration and separation of microalgae from water. The duration of this step ranges from a day to 10 days depending on the separation method (Qari et al., 2017). The choice of the harvesting method is based on the properties of microalgae such as size, density, concentration, and the value of the required byproduct (Brennan & Owende, 2010). The existing microalgae harvesting methods are categorized into biological, chemical, mechanical, and to a lesser extent, electrical operations (Branyikova et al., 2018)**,** as presented in Table 1. It is important to mention that harvesting of microalgae is considered as the most challenging step for algae industrialization due to the small size of the microalgae cell (< 30 µm) (Singh & Patidar, 2018) dilute nature of the microalgae culture (200 - 600 mg/L) (Christenson & Sims, 2011), and high operational cost which might exceed 50% of the total microalgae production cost (Milledge & Heaven, 2013). Microalgae harvesting technologies should be feasible with low energy requirement, minimize the addition of harmful chemicals, small footprint requirement, and provide the recycling of water medium (Laamanen et al., 2016). Introduction of electric field to conventional microalgae harvesting methods have shown great potentials to develop these methods. For instance, electro-flocculation and electrocoagulation processes are intensively employed for harvesting of microalgae due to their applicability on almost all microalgae species and sizes. Furthermore, no chemical or biological coagulants are required in these processes

because the coagulants are produced by electrolytic oxidation of metal electrodes with application of the electric field. Although of the high harvesting efficiency of these methods (80 – 95 %), however, the corrosion of the metal electrodes that contaminates the biomass, and the high energy requirement hinder the utilization of these processes (Singh & Patidar, 2018). The conventional harvesting methods of microalgae are reviewed and compared in chapter 2 section 2.1

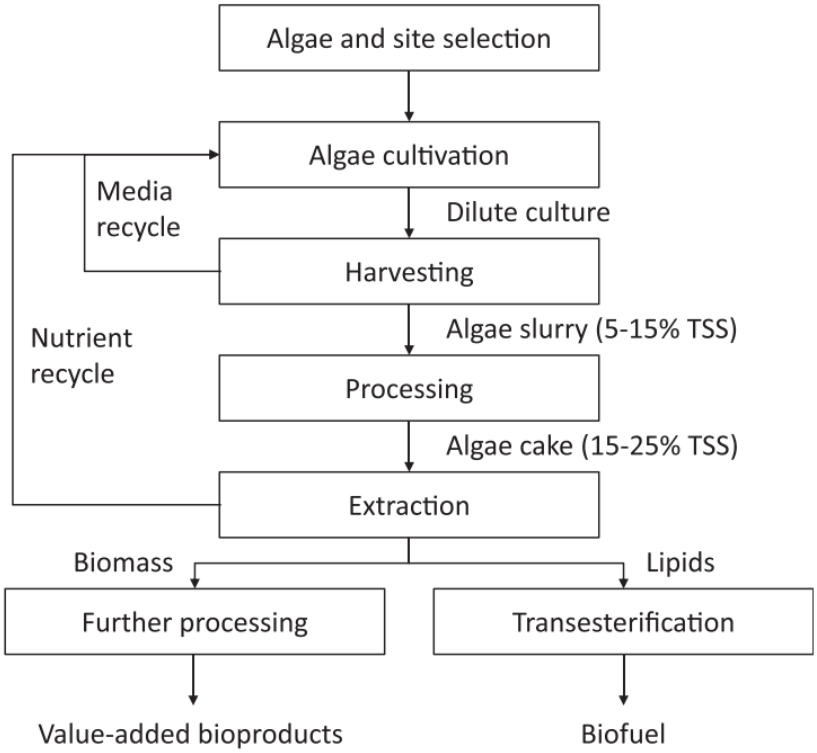

Figure 1. production stages of microalgae byproducts (Laamanen et al., 2016)

Table 1. Conventional Methods of Harvesting of Microalgae

Harvesting method	Technique used	Reference
Biological	Flocculation	(Ahmad et al., 2011)
Chemical	Coagulation-flocculation, flotation	(Branyikova et al., 2018)

Harvesting method	Technique used	Reference
mechanical	Sedimentation, filtration, centrifugation, flotation	(Drexler & Yeh, 2014) (Milledge & Heaven, 2013) (Garg et al., 2012)
Electrical	Electro-flocculation and Electrocoagulation	(Muylaert et al., 2017)

Among the electrical-based technologies, dielectrophoresis technique has shown potentials as an alternative for conventional microalgae harvesting methods. Dielectrophoresis technique have high selectivity for particles and cells manipulation. Dielectrophoresis is a highly selective particle manipulation technique, which is based on the motion of the dielectrically polarized particles by an inhomogeneous electric field (LaLonde et al., 2014), resulting in opposite but equal charges on both sides of the particle inducing a net force referred to as DEP forces. This force moves the particle to the weak or strong electrical field region based on the polarizability of the particle relative to the polarizability of the medium. Further explanation on the principal theory of DEP force and governing equations are provided in chapter 2 section 2.2.1. DEP force depends on variety of properties which are reviewed in chapter 2 section 2.2.2, providing multi-dimensional cell analysis.

The applications of dielectrophoresis technology (DEP) has shown satisfactory results as microalgae harvesting method, in terms of harvesting efficiency, energy consumption, and biomass contamination (Ho et al., 2017). The continues exploration and understating of the various factors that determine the DEP behavior of microalgae cells led to implementation of DEP for various applications such as trapping, deflection, concentration, sorting, and separation of microalgae. In addition to employing innovative designs and device geometries. Figure 2 below shows the increase in the

number of research related to the applications of DEP force to microalgae. Although of the increased attention in harvesting of microalgae using DEP, this technology is facing some drawbacks that limits the feasibility and applicability. The recent studies on harvesting of microalgae using dielectrophoresis has been conducted on small micro-scale. The small micro-scales may have high separation efficiency, but on the expense of low throughputs (i.e., below 1 $mL.h^{-1}$) that are only suited for handling very small samples (i.e., bench scale). Furthermore, most of these studies showed biomass contamination due to electrodes corrosion, or high energy requirement due the application of electric field, and other associated issues such as increase in temperature of the system. Therefore, further studies to enhance the operational conditions and overcome the aforementioned drawbacks are required.

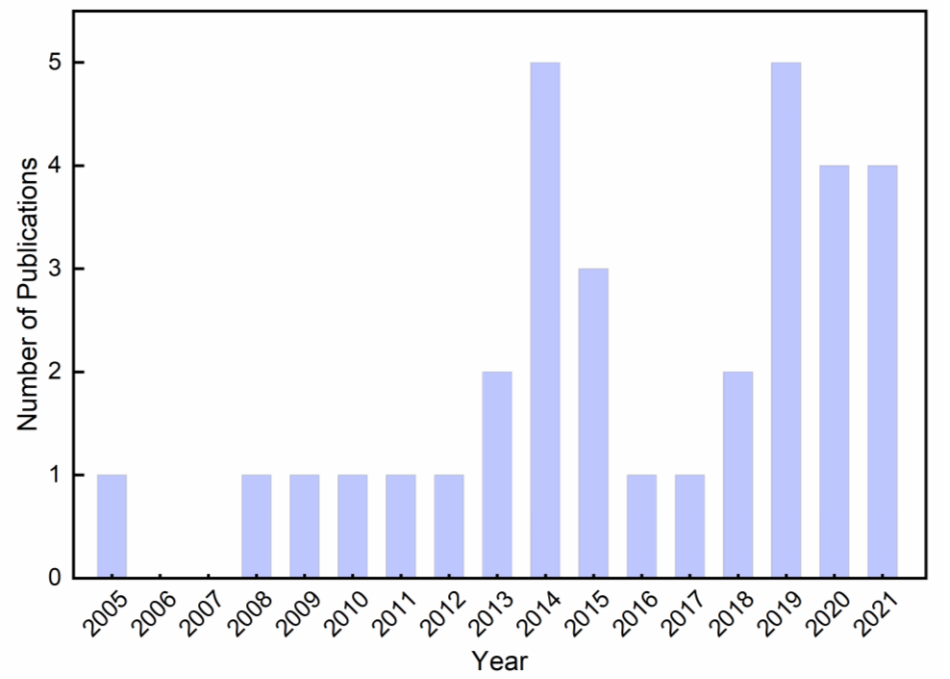

Figure 2. Number of publications on the application of DEP force on microalage.

1.2 Research Contribution

In literature, several studies have investigated the harvesting and separation of microalgae from water using dielectrophoretic force. Most of these studies have been conducted on micro-scale level and focused on developing the design and structure of microfluidic device and electrodes configuration. Other studies have investigated the impact of electric field properties such as applied voltage and applied frequency on particles trajectory and motion. However limited studies have addressed and solved the problems associated with miniaturization of dielectrophoretic separation systems. The very small sample target in the range of microliters (µL) to few milliliters, the increase of the medium temperature leading to reducing separation efficiency, and high energy requirement limit the process feasibility. Also, no studies have investigated the contamination of the harvested biomass with heavy metals due to electrodes corrosion. Therefore, this research study is investigating the harvesting of microalgae *Chlorella* sp. from freshwater medium at bench-scale using titanium dioxide (TiO_2) insulated electrodes inducing DEP force. Titanium dioxide insulation is used to prevent the accumulation of metals on the harvested biomass. Furthermore, to enhance the harvesting efficiency of microalgae, the effect of applied voltage and interelectrode distance on the intensity of the DEP force is investigated theoretically and proved experimentally. Also, to achieve high separation efficiency without sample disturbance, pulsed voltage and settling time experiments were added. The pulsed electric field is applied to minimize joule heating effect in the reactor. The optimal experimental conditions in terms of microalgae harvesting efficiency and energy consumption were found, including settling time, interelectrode distance, applied voltage, applied frequency, and pulsed DEP.

1.3 Research Objectives

The overall objective of this work is to study the harvesting efficiency of green microalgae cells by dielectrophoretic force at a macroscale level. This is achieved by investigating the following sub-objectives:

- To utilize a novel titanium dioxide (TiO_2) insulated stainless steel electrodes with interdigitated configuration for the separation of microalgae cells from the harvesting medium (freshwater) at a macroscale level.
- To simulate and study the effect of applied voltage and interelectrode distance on the intensity of DEP force.
- To study the effect of the experimental parameters including settling time, interelectrode distance, applied voltage, pulsed DEP and applied AC current frequency on the harvesting efficiency of microalgae cells.
- To study the feasibility of the process in terms of energy consumption and find the optimal operating conditions in terms of harvesting efficiency and energy consumption.

Chapter 2: Literature Review

2.1 Conventional Method for Harvesting of Microalgae

Commonly, the harvesting of microalgae takes place in doubled stages including:

1- Bulk harvesting: which is a large-scale process that aims for the separation of microalgae biomass from the bulk medium. This stage concentrates the biomass by 100-800 times and produce a solid slurry of 2-7%, depending on the microalgae initial concentration and methods utilized (Laamanen et al., 2016). The harvesting methods in this stage include flocculation, flotation, and gravity sedimentation.

2- Thickening: this stage aims to concentrate the slurry to more paste like with a concentration factor of 10-30 times. The methods employed in this stage include centrifugation, filtration, and ultrasonic aggregation. This stage requires more energy hence operational cost than the bulk harvesting (Barros et al., 2015).

With double-stage harvesting of microalgae, the diluted cell suspension of 200-600 mg/L can be preconcentrated to 10-50 g/L, and further treatment can reach the dry matter content to 25% w/v (Branyikova et al., 2018). Table 2 represents a comparison between conventional microalgae harvesting methods based on biomass recovery % and dry mass content after harvesting. The mentioned conventional methods often suffers from high energy consumption, long processing time and biomass contamination (Li et al., 2019; Whitton et al., 2015). Therefore, development of a harvesting process with high recovery of microalgae biomass, low energy consumption, with no byproducts produced is required to be considered for larger scale applications.

Table 2. Comparison Between Conventional Microalgae Harvesting Methods (Branyikova et al., 2018; Cheruvu et al., 2016; Laamanen et al., 2016; Milledge & Heaven, 2013).

Method	Recovery %	Dry solid content after harvesting %	Energy requirement	Advantages	Drawbacks
Centrifugation	> 90	12 - 22	0.5 kWh/kg	No chemicals. High-dry solid content. High biomass quality.	Energy intensive. Cell composition changes. High investment cost.
Gravity sedimentation	10 - 90	0.5 – 3	0.1 kWh/m^3	Cost effective. Suitable for bulk harvesting stage. Low energy requirement. Low cost of subsequent stages	Time requirement. Cell composition changes. Algal species specific.
Flotation	50 – 90	3 -6	—	Various options of filters. Reliable. Suitable for fragile cells.	Electrical flotation: electrode replacement, energy requirement.
Filtration	70 – 90 UF and MF ~ 100	5 – 27	0.169 kWh/kg of dry biomass	Suitable for shear sensitive algae. No chemicals. No contamination of the biomass. Ability for reuse of medium.	Membrane fouling and cleaning. Operational cost for membranes and pumps.
Flocculation and coagulation	> 90	2 - 7	Low energy required for slow mixing	Economically feasible	Electrical flocculation: energy requirement. Cell composition changes. Electrode fouling. Flocculant cost. Chemical flocculation: potential contamination.
Electrical-based methods	80 - 95	—	Very high	Applicable to all microalgal species. No chemicals.	Requires metal electrodes. Biomass contamination. Energy intensive.

2.1.1 Filtration

Filtration method employs a permeable separator for the separation of microalgae from water (Mata et al., 2010). Commonly, the driving force for the filtration process of microalgae is pressure or vacuum. Depending on the characteristics of the permeable separator such as pore size, most microalgae cells are retained while some cells might pass with the fluid into the filtrate (Muylaert et al., 2017). The choice of the permeable separator depends mainly on the microalgae cell size or molecular weight (Drexler & Yeh, 2014). The most studied and applied separators are the membranes such as microfiltration (pore size 0.1 – 10 μm), and ultrafiltration (pore size 0.001 – 0.10 μm) (Mustafa et al., 2014). Microfiltration membrane is used for larger microalgae cells (pore size > 10 μm) (Drexler & Yeh, 2014). Microfiltration and ultrafiltration membranes are more suitable for small scale applications (Mata et al., 2010). Another type of filtration is the screening of larger sized algae such as *Cyanobacteria Spirulina* (1–10 μm) (Carmichael et al., 2000). Screens are utilized to harvest algae in situ and are usually fabricated of nylon. Table 3 summarizes the studies on harvesting of microalgae using filtration processes.

Table 3. Summary of The Studies on Harvesting of Microalgae Using Filtration Processes.

Filtration process	Filter	Microalgae	Conditions	Efficiency	Reference
Pressure filtration	Ultrafiltration membrane	*Phaeodactylum tricornutum*	BC = 3.7×10^6 cells/L $t_{harvesting}$ = 1h	Concentration factor = 10	(Ríos et al., 2012)

Filtration process	Filter	Microalgae	Conditions	Efficiency	Reference
Pressure filtration	Submerged microfiltration	*Chlorella vulgaris*	pH = 8.5 BC = 0.41 g $_{\text{dry weight}}$ /L	Harvested TSS = 98 %	(Bilad et al., 2012)
Vacuum filtration	non-precoat vacuum drum filter	*Coelastrum proboscideum*	—	Harvested TSS = 18 %	(Molina Grima et al., 2003)
Vacuum filtration	suction filter	*Coelastrum proboscideum*	—	Harvested TSS = 8 %	(Molina Grima et al., 2003)

2.1.2 Centrifugation

Centrifugation is a gravity-based technology, and it is considered as the most robust, conventional, and widely used technology for harvesting of microalgae (Xia et al., 2017). The types of industrial centrifuges used depend on the biomass solid content in the water medium (Muylaert et al., 2017). For mediums with small biomass solid in the range of 0.01 – 20 %, disc bowel centrifuges are used. While for larger solids content from 10 – 50%, decanter centrifuges are used (Milledge & Heaven, 2013). Other types of centrifuges are disk-stack, nozzle discharge , and continuous flow centrifuges (Barros et al., 2015). Centrifugation is usually employed in the thickening stage of microalgae harvesting after flocculation, sedimentation, flotation, or membrane filtration, due to its ability to produce thick paste with high dry solid content. Table 4 summarizes the studies on harvesting of microalgae using centrifugation process. Centrifugation is considered the most energy requiring harvesting method with an energy consumption of approx. 3000 kWh/t (Xia et al., 2017).

Table 4. Summary of The Studies on Harvesting of Microalgae Using Centrifugation Processes.

Microalgae	Centrifuge type	Efficiency	Reference
Scenedesmus sp. and *Coelastrum proboscideum*	Disk-stack	Concentration factor = 120	(Molina Grima et al., 2003)
Nannochloropsis sp.	Continuous flow	Resulting TSS = 96	(Dassey & Theegala, 2013)

2.1.3 Coagulation - flocculation

Coagulation-flocculation methods is based on destabilizing microalgae cells suspended in water by neutralizing their negative surface charge and overcoming the electrostatic repulsion forces (Branyikova et al., 2018). Then allowing Van der Waals forces to attract and aggregate cells together and form larger flocs by the addition of flocculants (Mata et al., 2010). The coagulation-flocculation can be chemical using inorganic or organic agents, alkaline flocculation, bio-flocculation using microorganisms, or electrolytic flocculation (Xia et al., 2017). The most widely used coagulants are the inorganic metal salts such as $Al_2(SO_4)_3$ and $FeCl_3$ (Muylaert et al., 2017). Chitosan is used as an organic coagulant due to its abundance in nature and its strong ability for charge neutralization (Ahmad et al., 2011). Bio-flocculation is when some microalgae tend to flocculate spontaneously, or with presence of other microorganisms (Muylaert et al., 2017). Another form is auto-flocculation, which is based on pH changes induced by the precipitation of materials in water medium or by the microalgae surface changes (Laamanen et al., 2016). The increase in the pH of the medium will result in rapid aggregation of algae cells. This methods assist in easing the separation of these flocs by filtration or gravitational sedimentation and minimizing the

energy required for the subsequent stages (Molina Grima et al., 2003). Table 5 summarizes the studies on harvesting of microalgae using coagulation-flocculation processes. Coagulation-flocculation method combined with sedimentation or flotation is considered the most economic feasible bulk harvesting method (Brennan & Owende, 2010).

Table 5. Summary of the Studies on Harvesting of Microalgae Using Coagulation-Flocculation Processes.

Method	Coagulant	Microalgae	Conditions	Efficiency	Reference
Chemical coagulation	Chitosan	*Chlorella vulgaris*	pH 6.0 CD = 30 mg/L $t_{harvesting}$ = 10 min	92 %	(Rashid et al., 2013)
Chemical coagulation	$Al_2(SO_4)_3$	*Phaeodactylum tricornutum*	pH = 5.9 CD = 0.27 kg/kg $_{biomass}$ BC = 104.62 mg $_{dry\ weight}$	83 %	(Şirin et al., 2012)
Electro-flocculation	—	*Tetraselmins* sp.	pH = 8.4 I = 1.33 A CD = 100 A/m^2 $t_{harvesting}$ = 5.75 min	87 %	(Lee et al., 2013)
Auto-flocculation	pH adjustment NaOH	*Chlorella vulgaris*	pH = 10.8 BC = 0.5 g $_{dry\ weight}$ /L CD = 9 mg/g $_{biomass}$	98	(Vandamme et al., 2012)
Bio-flocculation	*Aspergillus oryzae*	*Chlorella vulgaris*	pH = 4.5 -7 $t_{harvesting}$ = 3 days	97 %	(Zhou et al., 2013)

2.1.4 Sedimentation or gravity settling

This method depends on the gravitational force to settle the microalgae particles and form concentrated slurry and an almost clear water medium (Pragya et al., 2013). Sedimentation is achieved using settling tanks such as inclined settlers or lamella separators which consist of a series of stacked plates (Muylaert et al., 2017). Sedimentation rate of microalgae depends on their cell size and the difference in cell density compared to the medium. the average microalgae cell size is less than 20 μm and the density of the cell is in the range 1.0 – 1.2 kg/m^3, therefore microalgae cells have very low settling rate of 1 cm/h (Milledge & Heaven, 2013). Sedimentation is usually employed for the bulk harvesting of microalgae because it produces dilute biomass slurry to an extent (Branyikova et al., 2018). Therefore, sedimentation is usually coupled with centrifugation, filtration, and mostly flocculation (Laamanen et al., 2016). Table 6 summarizes the studies on harvesting of microalgae using sedimentation process.

Table 6. Summary of The Studies on Harvesting of Microalgae Using Sedimentation Processes.

Microalgae	Method	Conditions	Recovery	Reference
Chlorella vulgaris	Gravity sedimentation	The density of which varied between 0.620 and 0.820 OD at 685 nm, $t_{harvesting}$ =1 h	60 %	(Ras et al., 2011)
Chlorella minutissima	Flocculation followed by sedimentation	1g/L of $Al_2(SO_4)_3$ $t_{harvesting}$ = 1.5 h, and $ZnCl_2$ $t_{harvesting}$ = 6 h	60 %	(Papazi et al., 2010)

2.1.5 Flotation

Flotation utilizes dispersed micro-air bubbles to attach to the cells and destabilize them hence cause them to rise and concentrate at the surface (Wang et al., 2008). Flotation method usually does not require the addition of chemicals however this result in low separation efficiency of 10% (Teixeira & Rosa, 2006). Therefore, coagulants are added to destabilize microalgae surface cells, which have negative surface charge (Wiley et al., 2009). The addition of coagulants will neutralize the surface and make the cells more hydrophobic resulting in flotations of the cells on the surface of the medium, hence increase the harvesting efficiency. The hydrophobicity of microalgae cells hence the harvesting efficiency increase with increasing the coagulant concentration (Garg et al., 2012). The common flotation types are dispersed air flotation (DiAF), dissolved air flotation (DAF), and electrolytic flotation (EF) (Laamanen et al., 2016). DiAF is the introduction of air by a diffuser such as agitator or porous medium (Uduman et al., 2010). The main limitation of using DiAF is the large bubble size which reduces the harvesting efficiency of microalgae (Hanotu et al., 2012). DAF depends on reusing the water medium which has been through the separation process. This water is pressurized to 400-650 kPa then depressurizing back to atmospheric pressure, consequently releasing air bubbles (Jarvis et al., 2009). EF is the process where the electrodes dissolves and forms coagulants that destabilize the microalgae hence form flocs. These flocs adhere with the air bubbles generated with electrodes dissolving and cause the microalgae flocs to float (J. Kim et al., 2012). Table 7 below summarizes the studies on harvesting of microalgae using different types of flotation process. Flotation has potential for more efficient separation compared to sedimentation (Edzwald, 1993), due to the tendency of microalgae cells to float rather than to precipitate (Phoochinda & White, 2003). The main drawbacks of flotation methods is the difficulties in process

engineering mainly at larger scale, and the limiting evidence of the technical and economic feasibility of the method (Laamanen et al., 2016).

Table 7. Summary of The Studies on Harvesting of Microalgae Using Flotation Processes.

Flotation type	Microalgae	Coagulant	Flotation time (min)	Removal	Reference
dissolved air flotation	*Chlorella vulgaris* (5×10^5 - 5×10^4 cells/mL)	$Al_2(SO_4)_3$ (4.3 pg/cell)	10	94.8 %	(Henderson et al., 2010)
dispersed air flotation	*Scenedesmus quadricauda* (7.4×10^4 cells/mL)	Cetyltrimethylammonium bromide (40 mg/L)	20	90 %	(Y. M. Chen et al., 1998)
electrolytic flotation	*Microcystis aeruginosa* (0.55 – 1.55×10^9 cells/L)	Aluminum electrode (1 mA/cm^2)	__	100 %	(Gao et al., 2010)

2.1.6 Electrolytic methods

Electrocoagulation is a pretreatment process for the harvesting of microalgae from water and wastewater (Shi et al., 2017). It was reported that EC is highly efficient process compared to chemical coagulation and flocculation in terms of removal rate and operation simplicity (Fayad et al., 2017). The mechanism of harvesting of microalgae using EC consists of 1) metal ions dissolution from the electrodes due to the passage of current hence forming coagulants, 2) these ions destabilized the particles suspended in the aqueous medium by reducing the zeta potential 3) neutralization of the surface charge of the particles by flocs formation, 4) and finally removal of the flocs

by flotation or settling (Emamjomeh & Sivakumar, 2009). The energy consumption using EC process was satisfactory compared to centrifugation. The energy consumption of EC is approximately 0.3 to 2 kWh kg^{-1}, depending on the medium (Vandamme et al., 2011). This suggests that is favorable and attractive method for harvesting of microalgae. However, this might be a limitation facing the scaling up of the process due to the increased energy requirement (Khatib et al., 2021). Another electrolytic method is the introduction of DEP force to existing technologies such as electrocoagulation. DEP force was introduced in EC process and showed improved process efficiency in terms of removal of particles, electrodes corrosion and energy consumption compared to the conventional EC process without DEP (Hawari, Alkhatib, Das, et al., 2020). Another electrolytic method is electrophoresis where with application of the electric field, water electrolysis occurs, and hydrogen bubbles are generated. These bubbles stick to the negatively charged algae cells and form flocs which float on the water surface. Electrophoresis technique is similar to the electrical flotation but without the dissolution of metal coagulants (Pragya et al., 2013).

Table 8. Summary of The Studies on Harvesting of Microalgae Using Electrical-Based Processes.

Microalgae properties	Electrodes	Optimum electric field properties	Removal efficiency	References
Tetraselmis sp. and *Chlorococcum* sp.	pair of flat sheet stainless steel electrodes	DC U = 10 V $t_{harvesting}$ = 900 sec	*Tetraselmis* sp. = 99% *Chlorococcum* sp. = 98%	(Uduman et al., 2011)

Microalgae properties	Electrodes	Optimum electric field properties	Removal efficiency	References
Chlorella vulgaris	Al electrodes	DC $t_{harvesting}$ = 10 min I = 2.2, 4.4, 6.7 mA/cm^2	98%	(Shi et al., 2017)
Nannochloropsis sp.	Al electrodes	DC I = 2.9, 4.8, 6.7 mA/cm^2 $t_{harvesting}$ = 60 min	up to 99%	(Fayad et al., 2017)
Tetraselmis sp. (C= 300 mg/L)	asymmetric cylindrical aluminum electrode (d= 2.5 and 4.5 cm)	AC-DEP I = 7.1 mA/cm^2 $t_{harvesting}$ = 10 minutes *f* = 50 Hz	96.4%	(Hawari, Alkhatib, Das, et al., 2020)
Tetraselmis sp.	array of 8 cylindrical IDE configuration (d= 2.5 mm, s= 1 cm)	AC-DEP I = 20 mA/cm^2 T = 10 minutes	96.18%	(Khatib et al., 2021)

2.2 Principles of Dielectrophoresis

2.2.1 Theory

Generally, dielectrophoresis is defined as the motion of charged or uncharged particles in a nonuniform electric field (Çetin & Li, 2011). When a particle undergoes an electric field, the particle will polarize meaning that the positive and negative charges distribute on the opposite sides of the particles. Coulomb forces are experienced by the particles due to the electric field and have the same magnitude but opposite charges. In the case of uniform electric field, the net force is zero, hence no particle

movement (Pethig, 2017a). However, when the electric field is nonuniform, the Coulomb forces on the particle edges are not equal hence the particle will carry a net force (Lewpiriyawong & Yang, 2014). Consequently, dielectrophoretic force will rise and the particle will move (Pethig, 2017b). The time-averaged DEP force experienced by a spherical particle in an inhomogeneous electric field is given as (Wei et al., 2009; Zhang et al., 2019):

$$F_{DEP} = 2\,\pi\,\varepsilon_m\,r^3\,\mathrm{Re}\,[K_{CM}]\,\nabla\,|E_{rms}|^2 \quad (1)$$

Where r is the particle radius, ε_m is medium permittivity, $\nabla\,|E_{rms}|^2$ is the root mean square of the inhomogeneous electric field gradient, and Re $[K_{CM}]$ is the real part of Calusius-Massotti (CM) factor (Hawkins et al., 2020; Honegger et al., 2011). At high frequencies, the real part of CM factor depends on the permittivity of a particle ε_p in relative to the permittivity of the medium ε_m, and given as (Ozuna-Chacón et al., 2008):

$$K_{CM} = \left(\frac{\tilde{\varepsilon}_p - \tilde{\varepsilon}_m}{\tilde{\varepsilon}_p + 2\tilde{\varepsilon}_m}\right), \text{where } \tilde{\varepsilon}_m = \varepsilon_m - \frac{j\,\sigma_m}{\omega} \text{ and } \tilde{\varepsilon}_p = \varepsilon_p - \frac{j\,\sigma_p}{\omega} \quad (2)$$

While at low frequencies, K_{CM} factor depends mainly on the conductive properties of the particle and suspending medium, and given as (Pethig, 2013):

$$K_{CM} = \left(\frac{\sigma_p - \sigma_m}{\sigma_p + 2\,\sigma_m}\right) \quad (3)$$

Where $\tilde{\varepsilon}_p$ and $\tilde{\varepsilon}_m$ are the particle and medium complex permittivity respectively, which determines how well a medium or particle will polarize when in an electric field (Kim et al., 2019). j is the imaginary part given as $j = \sqrt{-1}$, σ_p and σ_m are the particle and medium conductivity respectively, ω is the angular frequency of the electric field (Abt et al., 2020).

When a charged particle is suspended in an electrolyte medium, charges in the medium accumulate at the medium/particle interface, hence forming an electric double

layer EDL around the particle (Figure 3a) (H. Zhao, 2011). The EDL consists of two main layers: outer layer and inner layer. The outer layer named as the diffuse layer which is a charge cloud at which the diffusion force balances the counter-charge attraction force. While the inner layer named as stern layer in which a tight attachment is occurring between the positive charges and the colloidal particles negative surface (Ramos et al., 2016). The net force exerted on the particle is zero and particle is suspended in the medium. With the application of electric field, migration and convection of the charges in the EDL cause polarization of the particle or the medium (H. Zhao, 2011). This phenomena is named as Maxwell-Wagner interfacial polarization (Çetin & Li, 2011). This interfacial polarization depends on the relative permittivity of the particle in the medium, and in turn determines the type of DEP force (negative or positive) and the direction (Mukaibo et al., 2018). When the permittivity of the medium is higher than the permittivity of the particle -meaning that total charges on the medium side of the interface is higher, hence medium is more polarizable than the particle- the particle experience nDEP with a direction toward weaker electric field region (Figure 3b). While when the permittivity of the particle is higher than that of the medium -meaning that total charges on the particles side of the interface is larger, hence particle is more polarizable than the medium- the particle experience pDEP and moves toward the stronger electric field region (Figure 3b) (S. Molla & Bhattacharjee, 2007). The real part of K_{CM} factor ranges from −0.5 to 1. From Equation 1, when particle experiences pDEP $K_{CM} > 0$, and when particle is experiencing nDEP $K_{CM} < 0$ (Kim et al., 2019). In cases where the particle permittivity is equal to the medium permittivity ($K_{CM} = 0$), the particle experiences no polarization and zero DEP force, and the frequency at which this occurs is called the cross-over frequency (Alnaimat et al., 2020). Particle motion

in continuous flows is affected by the hydrodynamic drag from the surrounding fluid flow and gravitational force and their effect increase with particle's diameter. Therefore, DEP force should overcome other forces to induce particle motion (Jubery et al., 2014), and that requires a threshold of electric field to be applied depending on particle's diameter. The magnitude of DEP force depends on the size of the particle, and the amplitude and frequency of the electrical signals (Yanjuan Wang et al., 2018), which is discussed in next sections.

The models suggested to explain particles polarization behavior are the Maxwell-Wanger-O'Konski (MWO) model and Poisson-Nernst-Planck (PNP) model. MWO model explains the particle polarization behavior based on double layer thickness and frequency. However, this model fails to explain the polarization behavior of particles with thicker double layer ($\kappa a >> 1$) and at low frequencies (i.e., frequencies << cross-over frequency f_{XO}) (Pesch & Du, 2020)**.** Poisson-Nernst-Planck (PNP) equations are simplified and applied on all double layer thicknesses and in wider range of frequencies. This model explains the particle polarization behavior based on not only the EDL thickness and frequency, but also based on the electric field intensity and concentration gradient (H. Zhao, 2011). Several reviews have explained the mathematical and numerical models for particles polarization, and for calculation of the DEP force acting on spherical and non-spherical, biological and non-biological particles. The reader is referred to these reviews for more thorough explanation (Jubery et al., 2014; Pesch & Du, 2020; Pethig, 2010, 2013, 2017b; H. Zhao, 2011)**.**

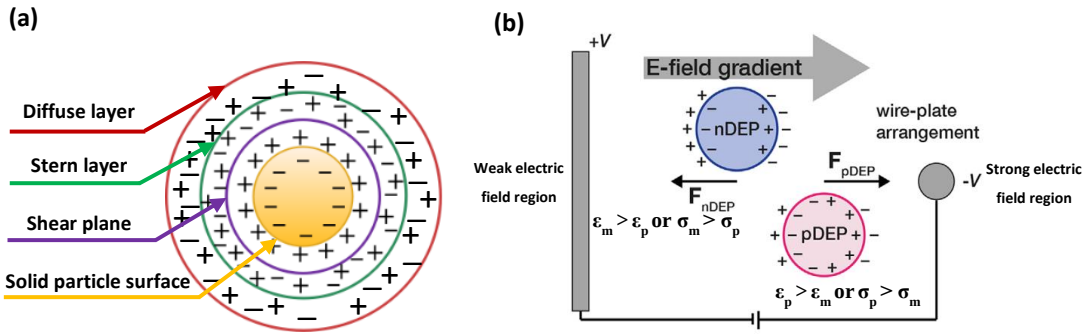

Figure 3. polarization behavior of a dielectric particles (Pesch & Du, 2020).

2.2.2 Factors affecting the dielectrophoretic separation

2.2.2.1 Polarization behavior of particles and cells

In aquatic dispersions, usually the medium (e.g., water or wastewater) has a very higher permittivity while suspended particles (e.g., cells, colloids, and solutes) have lower permittivity. Such differences in the permittivity of the medium and particles allow for DEP motion and hence implementation (e.g., capturing, concentration, sorting, or separation). Table 9 below represents the permittivity and conductivity of different types of water and wastewater media, and particles and cells suspended in these media. In this section, the polarization of conductive, non-conductive particles, and microorganism cells under wide spectra of frequencies is reviewed.

Non-conductive colloidal particles with diameter in the range of micro- and nano-meter show variation in DEP behavior at different frequencies and depending on the medium conductivity (H. Zhao, 2011). Since the conductivity of the bulk particle is low, the DEP behavior is completely dominated by the conductivity of the EDL formed under the influence of electric field. Therefore, due to the sufficiently high conductivity of the EDL surface (K_s) and the small particle radius (r), MWO model predicts that

such particles show pDEP at low frequency and nDEP at high frequency, at high medium conductivity (approx. 10^{-2} to 10^{-1} S/m). The pDEP behavior is expected at low frequencies when the particle radius is r < $\frac{2\,K_s}{\sigma_m}$ (Pesch & Du, 2020). A thorough investigation on the polarization behavior of non-conducting particles is reviewed by (H. Zhao, 2011). On the other hand, conducting particles (e.g., pure metals) have permittivity higher than the permittivity of the medium. Such particles show nDEP at low frequency up to cross-over frequency f_{XO}, where the net polarization is zero due to equal permittivity values of medium and particle (Midelet et al., 2019). At frequencies higher than the cross-over frequency f_{XO}, these conducting particles show pDEP behavior (Ramos et al., 2016). More thorough investigation on the polarization behavior of conducting particles is given in the review (Ramos et al., 2016).

For microorganisms, the dielectrophoretic response depends on the dielectric properties of the cell (i.e., permittivity and conductivity of cell wall, cell membrane, and cytoplasm). At low frequency, the DEP response of the cell is dominated by the conductivities of the cell and the medium. The low conductivity of the cell wall and membrane compared to the conductivity of the medium result in nDEP behavior (Gallo-Villanueva et al., 2011). At an intermediate frequency (i.e., beyond the first cross-over frequency f_{xo1}), the DEP behavior is dominated by the cell cytoplasm. The cytoplasm has higher conductivity than the medium, therefore it will polarize (reaching the maximum polarization at f_{peak}) resulting in pDEP behavior. At much higher frequencies (i.e., beyond f_{peak}), the DEP response of the cell is dominated by the permittivity of the cell and the medium. The insufficient time for cytoplasmic polarization (i.e., low permittivity) cause the pDEP to decrease, and with the high permittivity of the medium nDEP increase and represent the DEP behavior of the cell. The frequency at which the

pDEP decreases and nDEP increases is defined as the second cross-over frequency fxo_2 (Fernandez et al., 2017).

The differences in the permittivity and the conductivity of the mediums and the particles allow for diverse DEP responses in a wide range of electric field frequency. Therefore, with appropriately designed DEP device and electrode configuration as will be reviewed in next section, DEP technology could be implemented for particles capturing, concentration, sorting, rejecting, and separation.

Table 9. Dielectric Properties of Dispersion Mediums and Cells.

Medium/ Particle	Relative permittivity ε_p	Conductivity σ_p (μS/m)	Reference
Water	78-80	0.05 – 5	(S. Molla & Bhattacharjee, 2007; K. Zhao & Li, 2018)
wastewater	36 – 61.5	229×10^3 – 510×10^3	(Alkhatib et al., 2020; Bakır et al., 2019; A. H. Hawari, Alkhatib, Hafiz, et al., 2020)
Living cell wall	60	500 - 14×10^3	(Fernandez et al., 2017; Suehiro et al., 2003)
Living cell membrane	6	0.1 - 0.25	(Lapizco-Encinas et al., 2004a; Suehiro et al., 2003)
Living cell cytoplasm	50	2×10^5	(Suehiro et al., 2003)
Dead cell membrane	—	1000	(Lapizco-Encinas et al., 2004a)

2.2.2.2 Device and electrode configuration

The efficiency of particles manipulation by DEP force is significantly influenced

besides particle and mediums dielectric properties, by the electrode configuration and electric field strength. Due to the importance of the design of DEP device and electrodes configuration in inducing electric field inhomogeneity, numerous innovative device designs and electrode geometries have surfaced in the past decade, since the first separator invented by Pohl (Ballantyne & Holtham, 2010).

The working principle of DEP devices is based on either electrodes generating nonuniform electric field (i.e., electrode-based DEP), or obstacles distorting a uniform electric field to become a nonuniform field (i.e., electrodeless DEP) (Pesch & Du, 2020). In electrode-based DEP devices, bare electrodes or electrodes coated with insulating material are used. In electrodeless DEP devices, two types of obstacles are commonly used: insulator (iDEP) or metal (floating) obstacles (Pesch et al., 2016) to intensify the DEP force without having to increase the voltage. These obstacles could be used alone in the device such as in insulator based devices, or installed in between electrically excited electrodes (Pesch & Du, 2020). Insulators and insulation of electrodes is preferred in DEP devices to minimize electrodes corrosion, side electrochemical reactions, short circuit effects, and elevating risk of human electric shock of uncoated electrodes (Pesch et al., 2017). In addition, insulators retain their functionality despite surface fouling, and could be fabricated from various materials such as plastics or metal oxides. Using of plastics as an insulating material facilitates the fabrication of the device to handle higher flow rates (Ozuna-Chacón et al., 2008). DEP devices can be categorized based on sample throughput into low throughput (i.e., microfluidic chips $\mu L.min^{-1}$), and higher throughput (i.e., bench scale $mL.h^{-1}$).

In high throughput DEP system, the most common electrodes configuration

employed is interdigitated (horizontal) configuration (IDE) and oppositely installed (orthogonal) configuration (OPE). Figure 4 below represents the electrode configuration of DEP systems in combined water treatment applications. In IDE configuration, an array of electrically excited electrodes are placed opposite to each other with finger electrodes perpendicular on them (Figure 4a). Insulator obstacles could be placed between the finger electrodes to increase the inhomogeneity of the electric field (Y. Wang et al., 2015). In OPE configuration, two electrodes are installed on the two opposite sides of the system with fluid flowing in between (Figure 4b) (Y. Wang et al., 2014). IDE configuration provide more voltage across the medium hence intensified DEP forces compared to OPE configuration, considering identical energy consumption rates (Y. Wang et al., 2015). Therefore, it is the most employed electrodes configuration in water and wastewater treatment applications. The most common electrode or insulator shapes in high throughput applications are cylindrical, square, and circular shaped. Using square insulator at high voltage results in electric field higher in magnitude than using cylindrical insulator hence stronger DEP force. However, at lower voltage cylindrical insulator results in stronger electric field due to the difficulty of distributing the weak electric field homogeneously on the corners of the square insulator (Hawari et al., 2019; B Larbi et al., 2018). Furthermore, enlarging the diameter of the electrode cause stronger DEP force field compared to electrodes with smaller diameters.

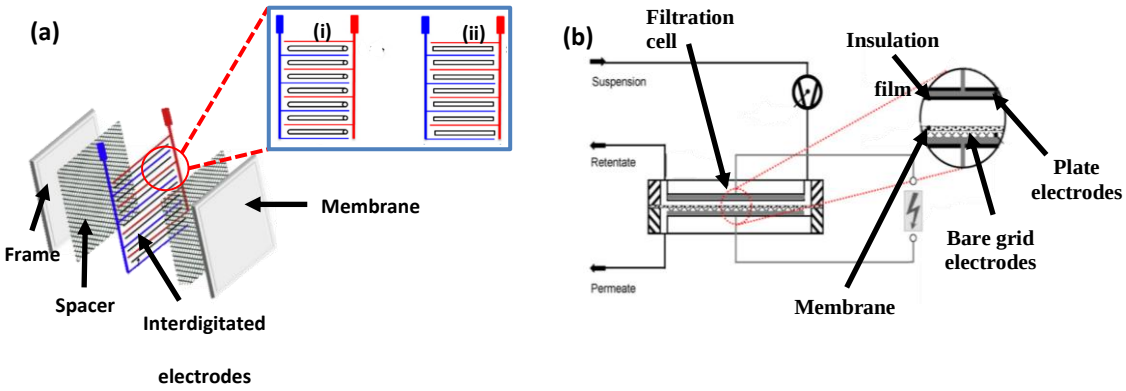

Figure 4. the design of DEP devices for high throughput applications (A. Hawari, Larbi, Alkhatib, Du, et al., 2019) (Du et al., 2009).

In low-throughput applications, microfluidic devices are utilized. The general structure of a microfluidic device usually consists of multiple layers; a layer of PDMS (polydimethylsiloxane) chamber, a layer of microfluidic PDMS channels or valves, and a third layer of microelectrodes or insulators placed on a glass substrate (Figure 5a) (Balasubramanian et al., 2007). Electrode configuration in electrode-based microfluidic devices that are reviewed in this paper can be categorized into external, two-dimensional, and three-dimensional electrodes (Zhang et al., 2019). The external electrodes are inserted into the sample inlet and outlet of the microchip, and with application of electric field the medium containing the target particles move from the inlet along the main channel and will be separated into different outlets (Figure 5b). The 2D electrodes are thin-film electrodes patterned at the bottom of the channel and based on simple fabrication methods. The most used 2D electrode configurations are parallel interdigitated and castellated electrodes. The most used 3D electrodes are metal electrodes and polymer electrodes (Zhang et al., 2019). In electrodeless devices, insulator-based DEP (iDEP) are the most common in microfluidic devices with

different insulator shapes and numbers used depending on the electric field intensity required for the application (Figure 5e).

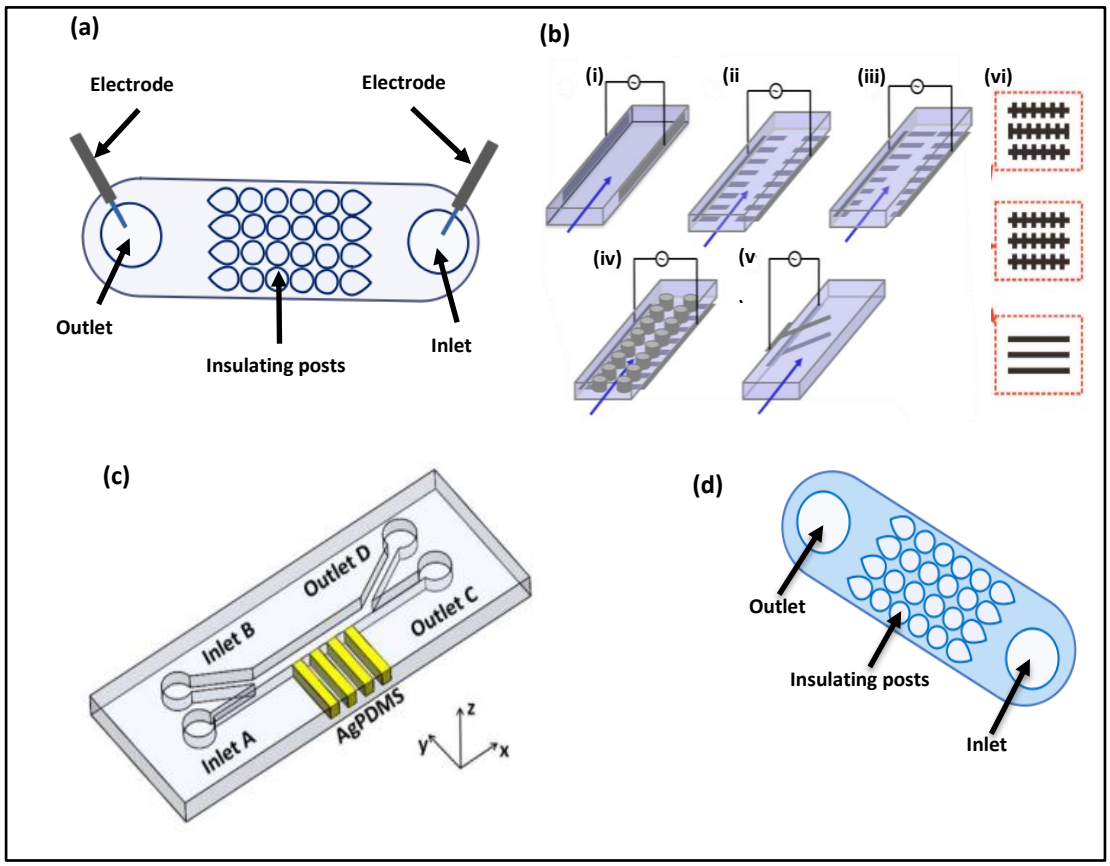

Figure 5. the designs of DEP microfluidic devices (a) external electrodes. (b) 2D-interdigitated and castellated electrode configuration. (c) 3D polyemer electrode configuration. (d) insulator-based microfluidic device (Yang, 2012) (Abt et al., 2020) (Zhang et al., 2019) (Jubery et al., 2014)(Saucedo-Espinosa & Lapizco-Encinas, 2015).

2.2.2.3 Electric field properties

In addition to device design and electrodes configuration, recent studies in DEP manipulation enhance the process efficiency by adjusting the electric field intensity. According to equation 1, the squared electric field $\nabla |E|^2$is directly related to the DEP force, thus stronger electric field result in stronger DEP force acting on the particles.

The intensity of the electric field increases with smaller distance between electrode and higher applied voltage. In addition to higher electric field strength around the electrodes in direct current (DC) electric field compared to alternating current (AC), under identical operating conditions (Yan et al., 2017) (B Larbi, Hawari, et al., 2017). However, stronger electric field in the system correlates with increase in temperature due to joule heating effect (Sridharan et al., 2011), thus limiting the application of DEP in aqueous mediums (Y. Wang et al., 2015). Elevating joule heating effect induce electrothermal flow (ACET) which is mainly due to the difference in water medium dielectric property (i.e., mostly conductivity) (Ren & Liang, 2020). Joule heating effect negatively impacts the viability of bioparticles and alters the physical properties of the medium (Hawari et al., 2019). Furthermore, the electrothermal forces introduce buoyancy forces that drives the medium and particles motion thus reducing the efficiency of particles capturing and separation (Du et al., 2009). Medium temperature is higher in the region near to the electrode resulting in lower fluid viscosity thus increase particles disturbance (Lapizco-Encinas, 2018). The optimum electric field for electrode-based devices is achieved at low voltages (approx. 10 V) and high frequencies, while electrodeless devices require higher voltages (approx. 1000 V) with application of DC, or low frequency with application of AC (Pesch & Du, 2020). According to (Hawari et al., 2015) sufficient DEP force is generated with application of high voltage, and lower energy is required with application of low frequency in electrode-based devices.

Using insulation of the electrodes leads to reducing the electric field intensity hence reducing the induced DEP force. Therefore, the thickness of the insulation film must be decreased. As the thickness of the insulation film decrease, greater high-pass-filter

effect (HPF) is developed. HPF allows only signals with high frequency to pass through the system (F. Du et al., 2009; F Du et al., 2013). Therefore, thinner insulation results in passing high critical frequency (f_{cr}), thus the voltage fraction (voltage across the medium U_m/applied voltage U_o) will increase leading to stronger DEP forces in the medium (Lapizco-Encinas, 2018). Using the metal (floating) electrode result in lower electric field compared to insulator obstacles. This is mainly due to more homogenous distribution of DEP forces in larger regions generated by insulator obstacles compared to metal floating metal electrodes (Fei Du et al., 2018).

2.3 Challenges of Dielectrophoretic Separation of Particles

Medium dielectric properties are the major challenge of dielectrophoretic separation of particles, due to its significancy in determining the magnitude and direction of the force hence target particle. A suitable medium for dielectrophoresis would be with a variable permittivity, low conductivity, and a high break-down threshold which is also safe and environmentally friendly. Water is an appropriate liquid medium to be utilized in DEP applications due to its economic feasibility and importance. However, due to the very high permittivity of water, the presence of dissolved ions that increase the conductivity, electrolysis of water that generates the turbulence, and consequently increasing in the energy requirement, applications of DEP in water are limited. (Ballantyne & Holtham, 2010) suggested that the high permittivity of water medium could be solved by changing the ratio of low permittivity and high permittivity liquids (i.e., mixing proportions of polar alcohols with non-polar hydrocarbons). However, water is immiscible with most hydrocarbons that can be used to lower the permittivity. In addition, these chemicals added should be safe,

environmentally friendly, and most importantly do not impact the target particles.

Most DEP-based studies show high selectivity and efficient particle trapping capabilities at the expense of low throughputs (i.e., below 1 $mL.h^{-1}$) that are only suited for handling very small samples (i.e., bench scale). A low throughput combined with a high selectivity is one of the general characteristics of contemporary DEP devices. Hence, to treat samples of preparative or industrial quantities, it is necessary to increase the throughput of DEP devices significantly. Increasing the throughput requires scaling-up the traditional DEP devices which in turn requires increasing the device dimensions, especially microfluidic channels size. However, knowing that the DEP acting on a particle decreases exponentially with increasing distance between the electrodes or from the insulating structures, therefore, the separation efficiency will decrease with increasing the device dimensions (Pesch et al., 2018). Consequently, scaling-up and increasing the throughput in traditional DEP devices will affect the separation efficiency (Lorenz et al., 2020). Electrodes fouling caused by high density of particles that experience pDEP after some time of continuous operation is an additional drawback. Electrodes fouling takes place particularly with application of high voltages and using bare metal electrodes.

In order to achieve more efficient treatment, particle separation techniques need to be capable of simultaneous manipulation of multiple particles especially particles with similar properties (e.g., diameter, permittivity, conductivity). The major drawback in dielectrophoretic separation is its ability to exert only pDEP and/or nDEP at a certain stage, thereby separating no more than two particle types at each stage. This shows the demand for a simultaneous multi-particle separation (Fernandez et al., 2017)

Joule heating effect generated from the application of AC or DC high electric field intensity is a major drawback (Calero et al., 2019). To overcome joule heating effect and impreove separation efficiecny, (Jubery et al., 2014) suugested the combination of electric conditions, such as AC and DC or the contactless DEP technique (cDEP). Because joule heating lead to decrease in the process performance at a certain threshold, a method to ehance the DEP selectivity and separation efficiency would be employing DEP field flow fractionation (DEP-FFF). DEP-FFF is a new variation of DEP technique which utilizes levitation and gravitational forces for separating the target particles. Another solution to overcome the joule heating problems even with application of high voltages is scaling-up DEP systems (Y. Wang et al., 2015).

Cell viability in another challenge of DEP separation of microorganisms. With the polarization of cells under the effect of a low frequency electric field, the cell membrane endures the electric field applied to the cell and shield the cytoplasm of getting polarized. Thus, the long duration of exposure to the electric field might lead to cell death depending on the conditions (Lalonde et al., 2015). A thourough investigation on the cell viability under electric field is found in the references (V. Wei et al., 2011)(Gallo-Villanueva et al., 2011) (Larbi, Ltaief, Hawari, Du, et al., 2017) (Lalonde et al., 2015).

2.4 Previous Studies on Harvesting of Microalgae by Dielectrophoretic Force

Several studies have investigated the harvesting of microalgae from water medium by dielectrophoretic force. Table 10 provides a summary on the studies of harvesting of microalgae using DEP microfluidic devices, and comparison in terms of

device design and separation efficiency. (Abt et al., 2020) reviewed 16 publications and studied DEP microfluidic devices categorized based on working principle and based on application type. Kumar et al., (2017) studied the dielectrophoretic response of green alga Coscinodiscus wailesii suspended in sterile seawater containing medium, in order to provide better knowledge on the impact of DEP force on the cells for water treatment applications. The microfluidic device consisted of an array of planar parallel surface gold electrodes with interdigitated configuration placed on both sides of the channel. The target microalgae cells were trapped easily to the side of the channel due to weaker fluid flow on the broadened sides of the channel and moved toward the electrode surface by pDEP. It was observed that microalgae displacement (µm) and velocity (in µm/sec) increased with increasing the applied voltage. While with applied frequency, the displacement and velocity of the cells reached the maximum at 10 kHz and decreased at higher frequencies. The low cell displacement and velocity at frequencies below 10 kHz is due to the high conductivity and salinity of the medium leading to air bubbles formation and sample disruption. The DEP force profile of microalgae cells was also studied, and it was found that the cells experience 4 times the magnitude of DEP force at the maximum applied voltage. On the other hand, the DEP force profile decreases at frequencies below the resonant frequency of 10 kHz and increase at the higher frequencies. This is due to the polarization behavior of the cells where at frequencies lower than 10 kHz, the time needed for the dipoles to charge/discharge is longer thus higher magnitude of DEP force exerted on the cells. The dielectrophoretic behavior of the green alga Tetraselmis sp was analyzed by application of traveling wave electric field to generate traveling wave DEP (twDEP), then used to estimate the dielectric properties of the cells (Bunthawin et al., 2012). Microelectrodes coated and

with IDE configuration were used. The green algal cells were cultured in artificial seawater medium. The results showed that as the medium conductivity increased the critical frequency was shifted towards higher frequency, while cell velocity spectrum was decreased significantly. At frequency range of 50 kHz - 0.5 MHz, the microalgae cells experienced pDEP, when increasing medium conductivity from 0.01 to 0.1 S.m-1. While at frequency range of 20 - 48 kHz, cells experienced twDEP with increasing medium conductivity from 0.01 to 0.37 S.m-1.

The effect of the structure of microfluidic chip and electric field parameters on microalgae separation efficiency was investigated. The capture and chaining efficiency of the green alga Chlamydomonas reinhardti and other phytoplankton cells suspended in freshwater using DEP microfluid chip was investigated (Siebman et al., 2017). A point needle electrodes configuration was used to collect and align cells in 2D structure. The chaining efficiency of microalgae increased with increasing the applied electric field intensity, applied frequency, and cell concentration. However, increasing the AC field duration for more than 5 minutes has no significant effect on the changing efficiency due to the low effective polarizability of microalgae. A maximum chaining efficiency of 80% of green microalgae was reached. Similar study was conducted by (Suscillon et al., 2013) for the capture of microalgae suspended in freshwater. Coplanar electrodes with parallels surface structure were used to collect and align cells in 1D arrays. The highest chaining efficiency of Chlamydomonas reinhardti achieved was 43% and 47.8 % suspended in freshwater from Geneva Lake and Laconnex Pond, respectively. It was found that increasing the electric field intensity, applied frequency, and AC field application duration result in significant increase in cell chaining efficiency. Moreover, no microalgae chains were formed at applied frequency lower

than 200 Hz, and disruption of cell chains was observed with applied frequency lower than 100 Hz. This is due to the AC electroosmosis fluid flow where the applied potential between the electrodes generates fluid flow which in turn disrupted the chain formation. The efficiency of cell chaining in freshwater samples (e.g., lake, pond, and river) was significantly affected by the chemical composition of the media and to some extent by the conductivity of the cells suspensions. Another study conducted by (Yanjuan Wang et al., 2018) on the on-site pretreatment of marine microalgae in ship's ballast water. A planar parallel surface gold electrode with interdigitated configuration was used for the continuous separation of microalgae Platymonas and Closterium microalgae. It was found that the triangular insulating structures between the electrodes increased the gradient of electric field intensity therefore, the two microalgae species in addition to polystyrene particles was efficiently separated into 3 different outlets. The DEP forces experienced by the two species of microalgae cells increased with the increase of the frequency of electric field. Closterium cells experienced nDEP at lower frequency and pDEP at higher frequency (higher than 1 MHz), while Platymonas cells experienced nDEP at all applied frequencies. It was also proved that increasing the amplitude of the applied voltage enhanced the separation, however further increasing in the applied voltage (more than 15 V) resulted in Platymonas cells to be mixed with the polystyrene particles and joule heating effect to be generated. Also, better separation efficiency was achieved with intermediate flow velocity of 0.01 mL/min. A maximum microalgae cells separation efficiency of 90% was achieved. Another study utilized planar parallel surface electrodes conducted by (Bahi et al., 2011), for the entrapment of marine microalgae Karenia brevis, in order to reach concentration enrichment of cells for RNA extraction and purification. The electrode configuration was interdigitated where arrays

of platinum electrodes placed facing each other. The interdigitated electrode configuration is efficient for DEP based cell trapping due to strong electric field generated which attract cells through a pDEP force.

Table 10. Summary of the Studies in Dielectrophoretic Separation of Microalgae Cells from Water Using Microfluidic Devices.

Medium and algae species	Device structure	Electric field [a]	Chaining efficiency	Reference
C. reinhardtii ($C = 3\times10^6$ cells·mL^1)	Microfluidic chamber (d = 350 µm), coplanar electrodes (Au, s= 2 mm)	AC-DEP E = 25 V.mm^{-1} *f* = 500 kHz t = 5 min	80 %	(Siebman et al., 2017) Done
C. reinhardtii	Microfluidic chamber (d = 250 µm), 2 coplanar parallel electrodes (Au, s = 2 mm)	AC-DEP E = 20 V.mm^{-1} *f* = 1 kHz t = 600 s	43-47.8 %	(Suscillon et al., 2013) done
Coscinodiscus wailesii	Microfluidic channel (PDMS, d= 125 µm, h= 250 µm), microelectrodes with IDE configuration (Au, d = 250 µm, s= 750 µm)	AC-DEP U = 10 V *f* = 10 kHz t = 60 sec	___	(Kumar et al., 2017) Done
Karenia brevis	Glass slide, Pt castellated interdigitated electrodes, gap between micro-electrodes were 20 µm	U = 1 V *f* = 0.2 MHz $\dot{V}$ = 0 µl·s^{-1}	____	(Bahi et al., 2011)

[a] The electric field applied to obtain the maximum DEP force, hence maximum concentration and separation.

Medium and algae species	Device structure	Electric field [a]	Chaining efficiency	Reference
Selenastrum capricornutum	Two chambers with different posts dimensions (470 and 520 µm), array of 32 insulating cylindrical posts arranged in eight columns and four rows	E = 100, 800 and 2500 V/cm f = 0	___	(Gallo-Villanueva et al., 2011)
Platymonas and *Closterium* cells in ballast water	Microchip (PDMS, ITO conductive layer), parallel IDE electrodes (Ag-PDMS mixture): a 3D rectangular electrode (L= 1900 µm, w= 2000 µm), and 8 discrete strip electrodes with sharp angles (w= 100 µm, s= 100 µm), separated by a 3D triangular insulated hurdle structure (d= 30 µm).	AC-DEP U= 10 V f = 30 MHz $\dot{V}$= 0.01 ml/min	___	(Yanjuan Wang et al., 2018) Done
Tetraselmis sp.	Microchip (L= 750 µm), octa-pairs microelectrode array with IDE configuration (w = 50 µm) coated (Au, d = 0.5 µm)	U = 1.5 – 14 V_{pp} f = 5 Hz- 4 MHz $\dot{V}$= 2.4 $\mu l \cdot s^{-1}$	___	(Bunthawin et al., 2012)

[a] The electric field applied to obtain the maximum DEP force, hence maximum concentration and separation.

Chapter 3: Materials and Methods

3.1 Cultivation of Microalgal Species (*Chlorella* Sp.)

Freshwater *Chlorella* sp. was collected from Qatar University Culture Collection of Cyanobacteria and Microalgae (QUCCCM). *Chlorella* sp. is a green microalga (unicellular) with cell size 2-8 μm. Figure 6 shows a microscopic image of the *Chlorella* sp. microalga. Initially, colonies of *Chlorella* sp. cells were taken from an agar plate and added to a 100 mL growth media in a 250 mL flask. The flask was transferred into an orbital shaker maintained at 120 rpm and 25 °C. The light intensity on the flask was 100 μmol E/m^2/s, and the light: dark period was maintained for 12h:12h. After 7 days of growth, this flask culture was transferred to a 1L glass PBR (8 cm dia). Air was sparged, at a rate 0.5 v/v/m, at the bottom of the PBR to provide sufficient mixing. Cool fluorescent lighting was used to provide a light intensity of 600 μmol E/m^2/s. After 7 days, the PBR culture was transferred to a 10 L plastic PBR and mixed with 9 L of growth media. The light intensity and the air mixing for the 10 L PBR were the same as used for the 1 L PBR. Autoclaved growth media was used for the flask and 1 L PBR growth. However, the freshwater used for the 10 L PBR was sterilized using 5 mL commercial bleach (15% chlorine). For all the cultivation, 78 mg/L urea and 10 mg/L sodium phosphate were used as sources of Nitrogen and Phosphorus, respectively, whereas all other nutrients had the same BG-11 media concentrations. The PBR cultures were periodically monitored for possible contamination by other microalgae/cyanobacteria. After 10 days of growth in the plastic PBR, the culture was used for the harvesting experiment. Figure 7 shows the microalgae samples suspended in freshwater. Table 11 below summarizes the characteristics and dielectric properties of the microalgae *Chlorella* sp. Cells and the medium suspension.

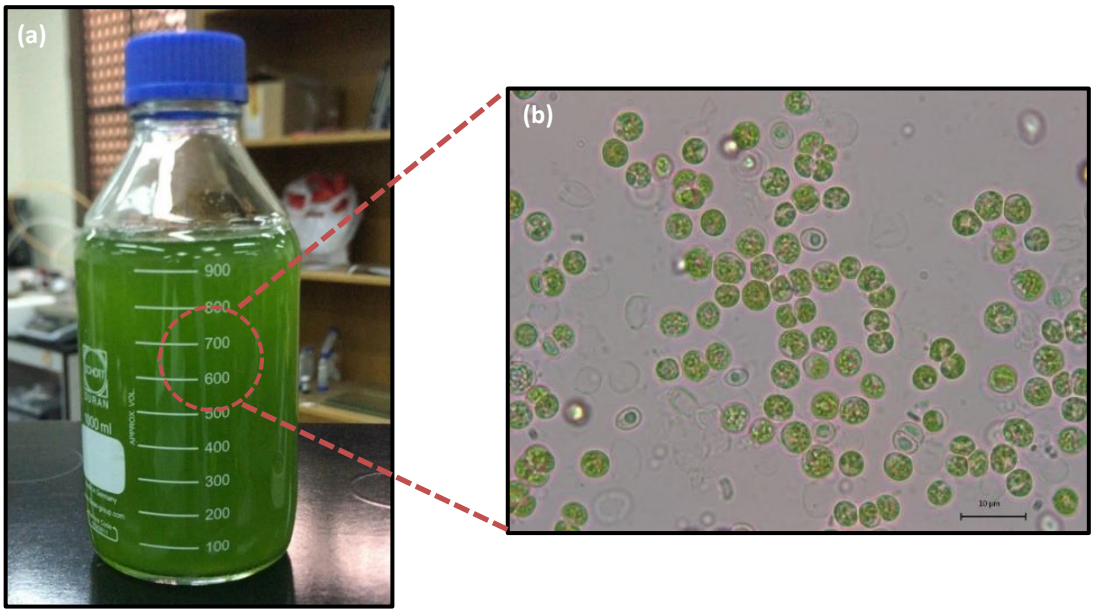

Figure 6. (a) Microalage suspended in freshwater medium and (b) microscopic image of the microalga *Chlorella* sp. Cells.

Table 11. Carcteristics and Dielectric Properties of The Microlagae *Chlorella* Sp. Cells and the Medium (Fernandez et al., 2017; Suehiro et al., 2003).

Microalgae category	green algae (unicellular)
Stain name	*Chlorella* sp.
Cell size	2 - 8 µm
Cell conductivity σ_p	80 – 500 µS/cm
Cell wall permittivity ε_p	60
Cell cytoplasm permittivity ε_p	50
Conductivity of freshwater and microalgae mixture σ_m	1-5 µS/cm
Relative medium permittivity ε_m	78.4-80
Zeta potential d ζ	-2.03×10^{-2} V
Double layer thickness	3.00×10^{-9} m

3.2 Experimental Setup

The experimental runs were conducted in a macroscale glass tube (length: 8 cm – diameter: 2.5 cm). Each tube contained 40 ml of the sample with a microalgae concentration of 103 ± 2 ppm. The harvesting of microalgae using DEP force was evaluated using two symmetrical aluminum electrodes (diameter: 0.2 cm - length: 12.4 cm - effective surface area: 0.63 cm^2). The electrodes were coated with 200 nm thin film insulating layer of hydrophobic titanium dioxide (TiO_2, rutile) in order to prevent

the contamination of the harvested algae sample by the electrode material. Titanium is preferred as an insulation film due to its high biocompatibility, specific strength, and corrosion resistance. Insulation of the electrodes was done by low atmospheric pressure chemical vapor disposition (CVD) technique. The electrodes were connected to an alternating current high pulse voltage generator (G2000, Redline Technologies, Baesweiler, Germany). The voltage and current were measured using an oscilloscope (MDO3024, Tektronix, Oregon, US). A peristaltic pump (FPU5-MT, OMEGAFLEX, PA, US) was used to collect the sample after the experiment. The temperature and pH were measured using multimeter (PCD650, OAKTON, US). The absorbance was measured with UV-VIS spectrophotometer (ORION AQUAMATE 8000, Thermo SCIENTIFIC, US) at wavelength of 750 nm. An overview of the experimental setup is illustrated as a sketch in Figure 8 and as picture in Figure 9.

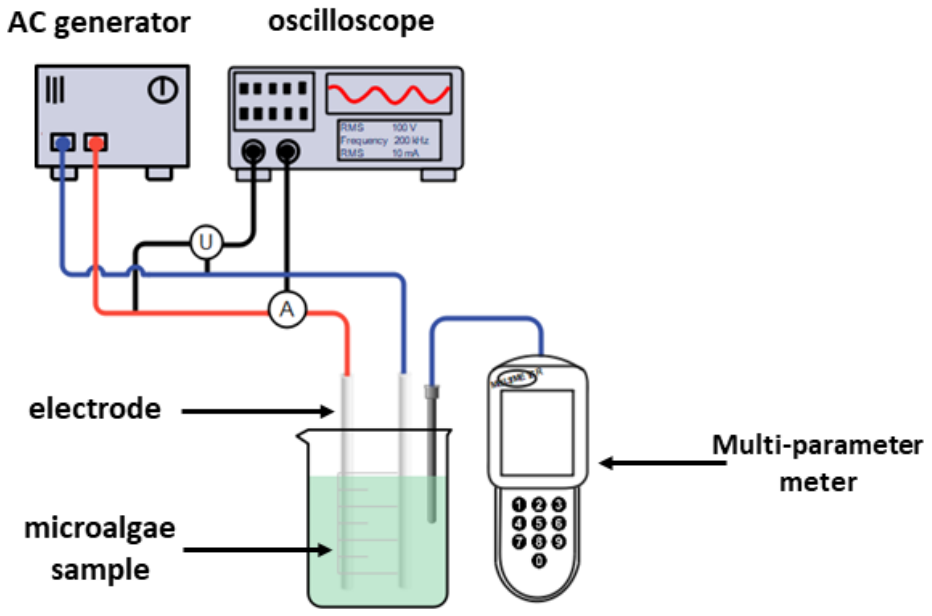

Figure 7. A schematic sketch for the bench-scale experimental setup.

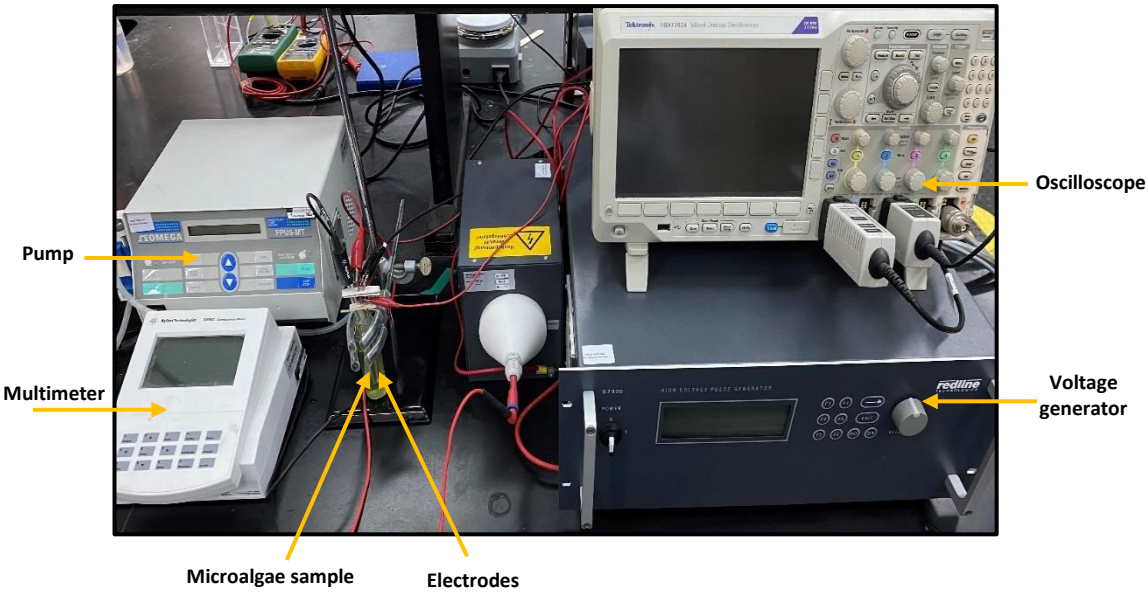

Figure 8. A picture for the bench-scale experimental setup.

3.3 Experimental Method

First, the microalgae sample was characterized by measuring the absorbance, pH and temperature using the spectrophotometer and multimeter. All experiments were carried out at an ambient temperature of 23 °C, and pH of 6.0 ±0.2. Second, the stability of the microalgae sample was tested by monitoring the settlement of the cells over time without applying electrical field. Third, the effect of settling time, interelectrode distance, applied voltage, and frequency were evaluated. Settling time of 0, 10, 30, 60 and 90 minutes were investigated at an interelectrode distance of 6 mm, voltage of 200 V and frequency of 150 kHz after 15 minutes application of DEP. Three interelectrode distances of 4 mm, 6 mm and 8 mm were evaluated at an applied voltage of 200 V and frequency of 250 kHz. Three different applied voltage values of 100, 150 and 200 V were studied at an interelectrode distance of 6 mm and frequency of 250 kHz. The effect of applied current frequency 50 Hz, 100, 150, 200, and 250 kHz were evaluated at an interelectrode distance of 6 mm, applied voltage of 200 V, and DEP application time of 20 minutes. The temperature and pH of the microalgae sample were monitored

during the experiment. The samples were collected from the reactor using a pump motor to minimize the disturbance of the sample. The microalgae harvesting efficiency was evaluated based on the difference in optical density of the microalgae between initial and harvested samples (at 750 nm) using Equation 4:

$$\eta = \left(\frac{OD_{initial} - OD_t}{OD_{initial}}\right) \times 100 \quad (4)$$

Where η is the harvesting efficiency of the microalgae (%), $OD_{initial}$ is the initial optical density of the culture medium and OD_t is the optical density of the culture medium at a certain time. The energy consumption (C_{Energy}) in kWh/kg of the harvesting process were calculated using the Equation 5:

$$C_{Enenrgy} = \frac{U \times I \times t}{1000 \times V \times C_i \times \eta} \quad (5)$$

Where U is the applied voltage (volt), I is the applied current (A), t is the electrolysis time (minutes), v is the microalgae biomass volume (m^3) and C_i is the initial concentration of the microalgae biomass (kg/m^3). To find the most suitable operating condition, the harvesting efficiency and energy consumption data sets were normalized using Equation 6. Then, the normalized harvesting efficiency was added to the inversed normalized energy consumption to select the most optimum running conditions.

$$\text{Normlized value} = \frac{(\text{value} - \text{min})}{(\text{max} - \text{min})} \quad (6)$$

3.4 Numerical Method

To study the effect of interelectrode distance and applied voltage on the DEP force in the proposed setup, a numerical model was built using COMSOL Multiphysics 5.5. As seen above in Equation 1, the DEP force is directly proportional to the square of the electric field. Thus, the square of the electric field was calculated as an indicator for the DEP force in the proposed electrode configuration. The schematic of the

simulated geometry consisting of two circular shaped aluminum electrodes coated with titanium dioxide is shown in Figure 10.

The electric potential was solved at a set of boundary conditions. To solve this problem for the current densities, the quasi-electrostatic form was used. The root mean square (rms) of the electric field is calculated using the equation (Du et al., 2009):

$$E = -\nabla \varphi \tag{7}$$

Where, φ is the root mean square of the electrostatic potential given by the Laplace's equation:

$$\nabla^2 \varphi = 0 \tag{8}$$

The boundary conditions were fixed for the surface of the charge carrying electrodes, where U_o is the root mean square of the oscillating potential drop:

$$\varphi_1 = U_o \tag{9}$$

$$\varphi_2 = 0 \tag{10}$$

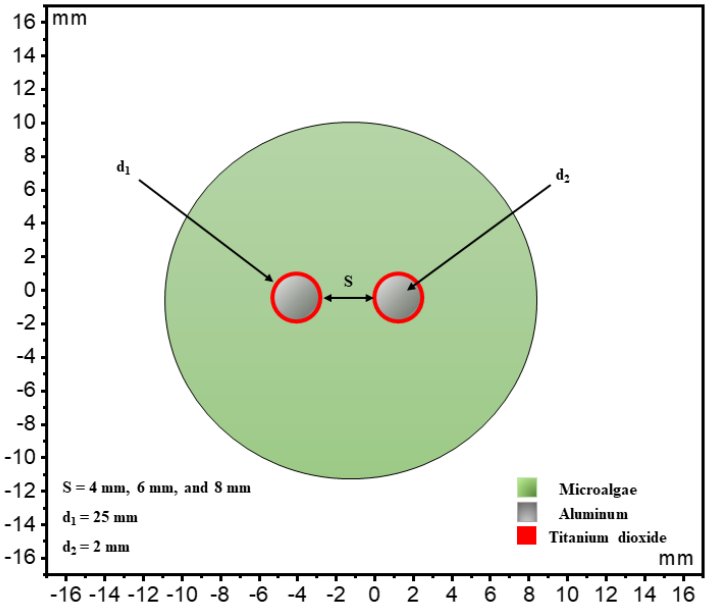

Figure 9. Illustration of the COMSOL model showing the geometrical parameters and the materials used in the numerical simulation.

3.5 Error Estimation

Harvesting process for each experimental parameter at every time range was repeated twice. The reported results are the average of the experimental trials. Error bars represents the standard deviation of the results. The following Equation was used to calculate the standard deviation error bars for each reported data:

$$SD = \sqrt{\frac{\sum_1^N (x_i - \tilde{x})^2}{N}} \quad (11)$$

Where, x_i is the measured value, $\tilde{x}$ is the average of the measured values, and N=2 which is the number of repeats. Error bars are shown on all Figures, and all error bars of the standard deviation do not exceed 3%.

Chapter 4: Results and Discussion

4.1 Effect of Settling Time on Harvesting Efficiency

The effect of different settling time on the harvesting efficiency of the microalgae after the application of the electrical field was evaluated. A settling time of 10, 30, 60, and 90 minutes were investigated. The interelectrode distance and applied voltage were kept constant at 6 mm and 200 V, respectively, for 15 minutes electric field application. The settling of microalgae in a control sample with no electric field was measured in order to ensure that harvesting of microalgae is completely due to the application of the electrical filed. As shown in **Error! R eference source not found.**11a, the harvesting efficiency without the application of the electric field is low and reached a maximum of 10% after 90 minutes. The tested microalgae cells are very small in size with a diameter ranging between 2 – 8 µm which made them stable in solution and hard to settle. The removal efficiency of the microalgae cells with the application of the electric field was 72.5% at zero settling time. It was noticed that while the electric field is on, most of the microalgae cells moved toward the strong electric field close to the surface of the electrodes due to pDEP force. After a period of time, it was noticed that the microalgae cells where entrapped between the two electrodes forming a pearl-chain effect as shown in Figure 11b. The pearl-chain effect occurs due to an induced dipole-diploe interaction between the microalgae cells which cause the cells to align in chains along the electric field (Du et al., 2013; Pethig, 2010; Wong et al., 2004). Once the electric field was turned off and after 10 minutes of settling the removal efficiency of the microalgae decreased to 46% due to the dispersion and resuspension of the microalgae cells into solution. As the settling time increased the removal efficiency increased to reach 69% after 90 minutes of settling time. With time and due to size enlargement and

agglomeration of the microalgae cells, these agglomerates settled by the influence of the gravitational forces as shown in Figure 11c. It was found that after 90 minutes settling time, the removal efficiency was high (i.e., 69%) almost similar to the initial 72.5% removal efficiency when the electric field was on. Therefore, in this study, a settling time of 90 minutes was applied for all samples after the application of the electric field.

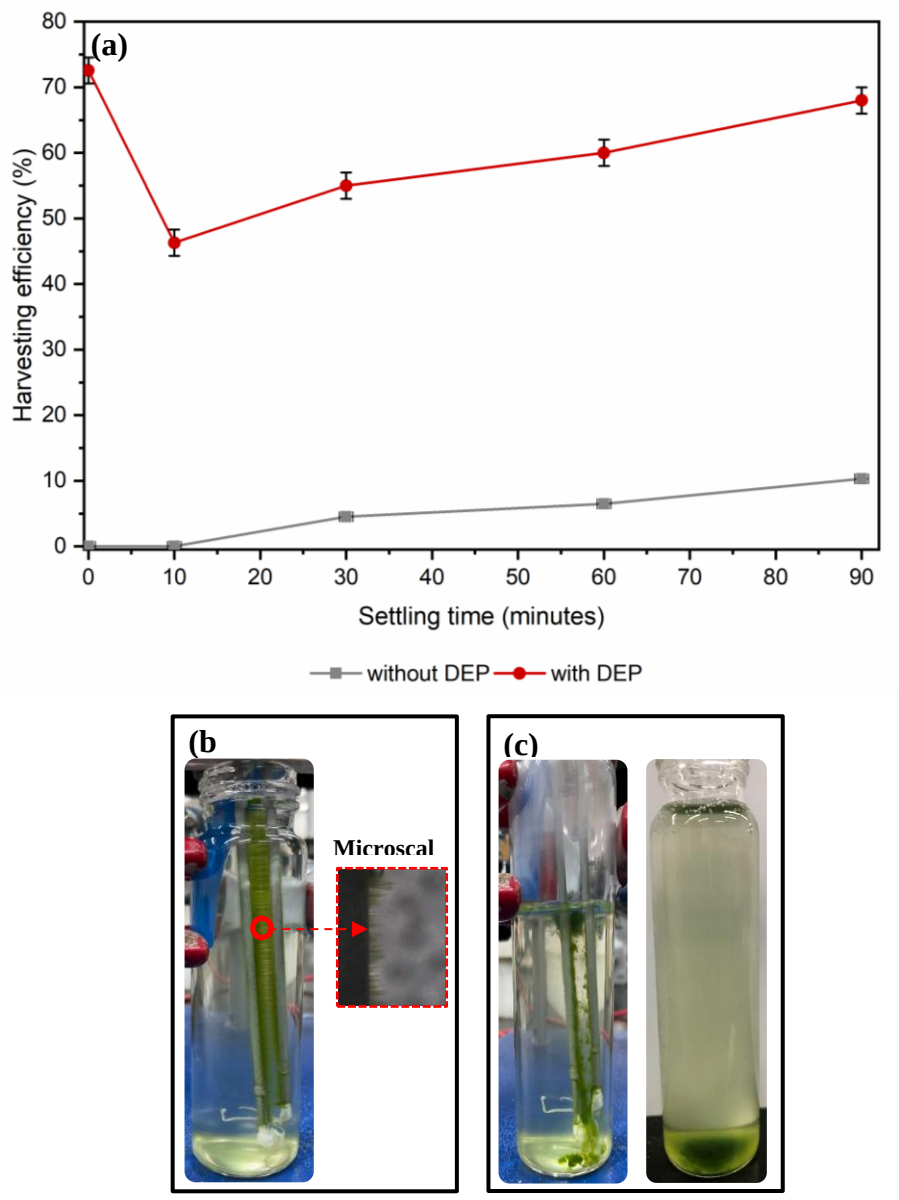

Figure 10. (a) effect of settling time on microalgae harvesting efficiency at the following conditions: without electric field and with electric field application using 200 V, 150 kHz, 6 mm, and 15 minutes (b) entrapment of most of microalgae cells between electrodes and pearl chain effect formation with the application of electric field (c) (left): resuspension of cells when electric field is turned off and large agglomerates formation, (right) settling of agglomerates after 90 minutes.

4.2 Effect of Applied Voltage on Harvesting Efficiency

The effect of voltage on the DEP force represented as the squared electric field $|\nabla E^2|$ was numerically evaluated. Then, the effect of applied voltage for different times on microalgae harvesting efficiency was experimentally investigated. The studied applied voltages were 100 V, 150 V, and 200 V with electric field application time of 5, 10, 15, 20, 25, and 30 minutes. The interelectrode distance and AC frequency were kept constant at 6 mm and 250 kHz, respectively. The DEP force field distribution was represented in **Error! Reference source not found.**11, and the i ntensity of the DEP force field increased with increasing the applied voltage form 100 V, 150 V, to 200. In Figure 12, the calculated value of the DEP force represented by the square of the electric field ($\nabla|E|^2$) was shown. The highest $\nabla|E|^2$ values were 1.89×10^{12}, 4.26×10^{12} and 7.58×10^{12} V^2/m^3 for an applied voltage of 100, 150 and 200 V, respectively. From Figure 11 and Figure 12, it can be stated that stronger DEP force field is present at the electrode surface with application of higher voltage, and the intensity of the DEP force field decrease with application of lower voltages. The increase in DEP force with increasing applied voltage indicate that higher harvesting efficiency should be obtained, which agreed with the experimental results shown in Figure 13. It was found that the harvesting efficiency of microalgae increased with higher applied voltage and longer application time reaching highest

values of 19.4%, 38.1%, and 63.9%, with applied voltages of 100 V, 150 V, and 200 V, respectively, after 30 minutes of application of the electric field.

The effect of applied voltage on the microalgae harvesting efficiency at interelectrode distances of 4 mm and 8 mm were also investigated. At small interelectrode distance of 4 mm, the harvesting efficiency of microalgae increased with the applied voltage of 100 V and 150 V, reaching the highest harvesting efficiency of 30.1% and 64.9%, respectively (Figure 14). This harvesting efficiency increased with increasing applied voltage due to the application of an electric field strong enough to capture microalgae cells. However, with application of higher voltage of 200 V, the harvesting efficiency of microalgae increased reaching the maximum of 70.4% after 20 minutes of application time. After 20 minutes, the harvesting efficiency kept decreasing reaching to 26.5% after 30 minutes. This is due to the joule heat effect which generates temperature gradient in the medium. The temperature gradient is higher in the strong electric field region between the electrodes, and lower temperature in the weak electric field regions away from the electrodes. This temperature gradient induces the fluid flow of the medium consequently resulting in disturbing of the harvesting process of microalgae. On the other hand, at larger interelectrode distance of 8 mm, the harvesting efficiency of microalgae increased with application of higher voltage and reaching to 11.8%, 14%, and 28% at voltage of 100 V, 150 V, and 200 V, respectively (Figure 15).

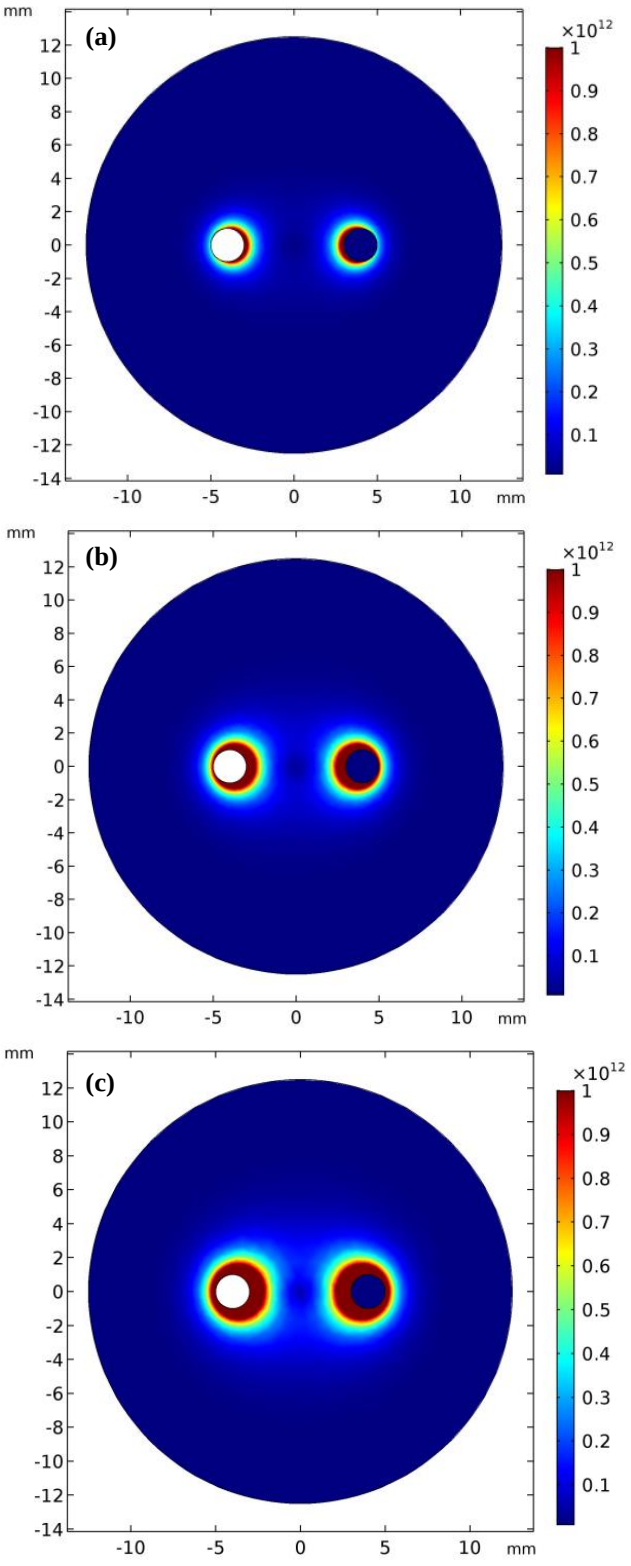

Figure 11. The DEP force field distribution defined as ($\nabla|E|^2$) for the applied voltages of (a) 100 V, (b) 150 V, and (c) 200 V, at interelectrode distance of 6 mm and frequency of 250 kHz.

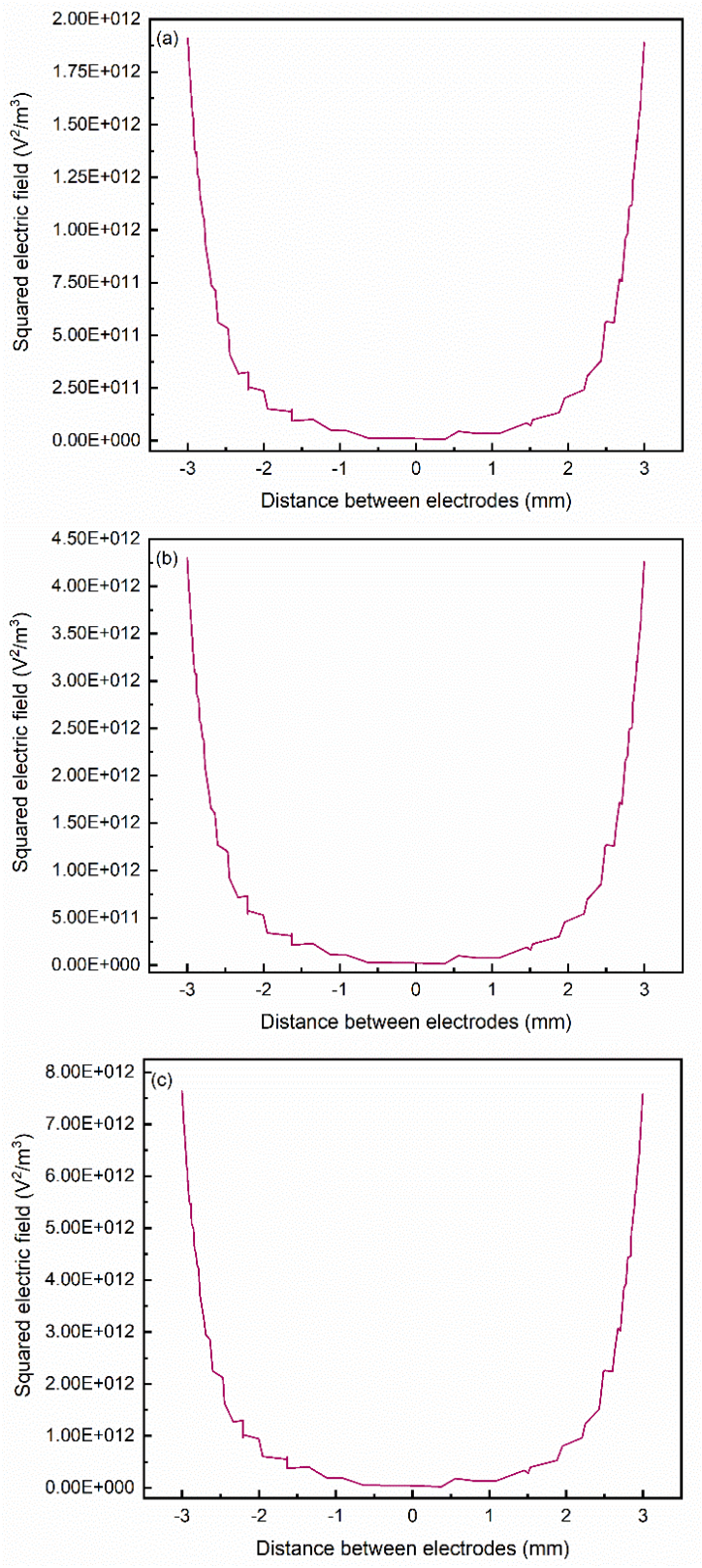

Figure 12. The calculated DEP force defined as ($\nabla|E|^2$) for the applied voltages of (a) 100 V, (b) 150 V, and (c) 200 V, at interelectrode distance of 6 mm and frequency of 250 kHz.

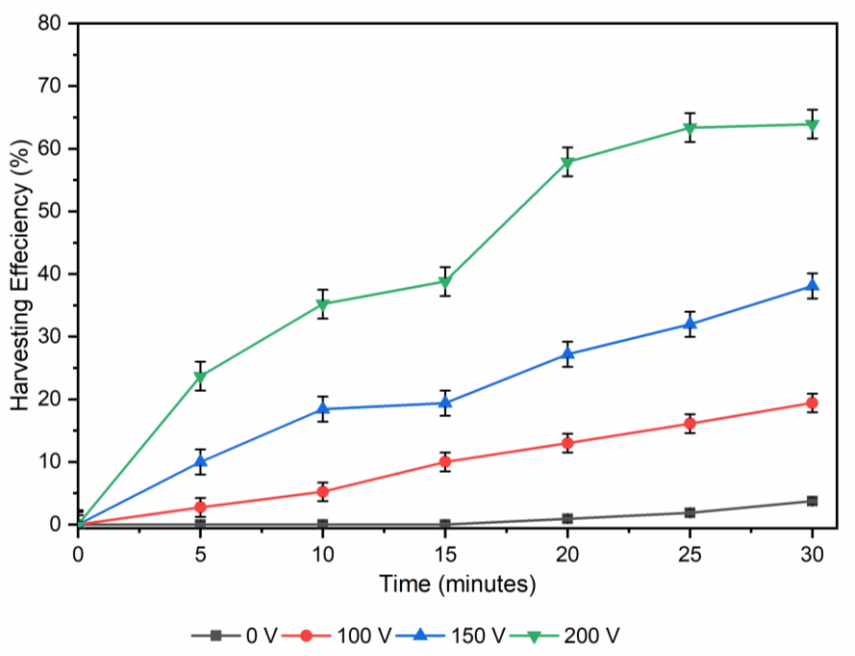

Figure 13. The effect of applied voltage on microalgae efficiency at an interelectrode distance of 6 mm and frequency of 250 kHz

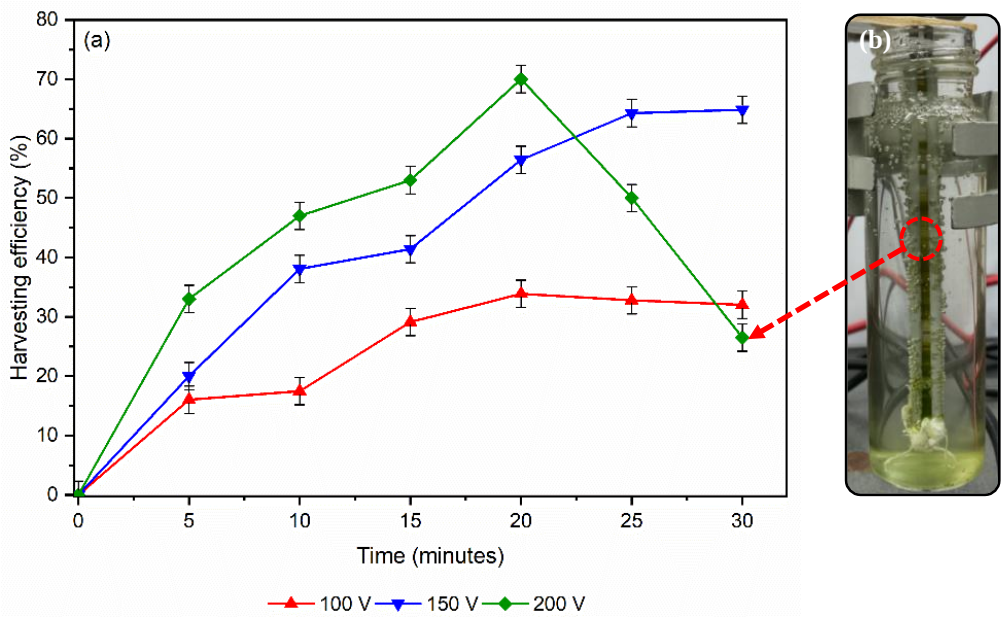

Figure 14. The effect of applied voltages on the harvesting efficiency at frequenscy of 250 kHz and interelectrode distance of 4 mm and (b) disturbamce of microlagae harvesting process due to electrothermal fluid flow induced by joule heating effect.

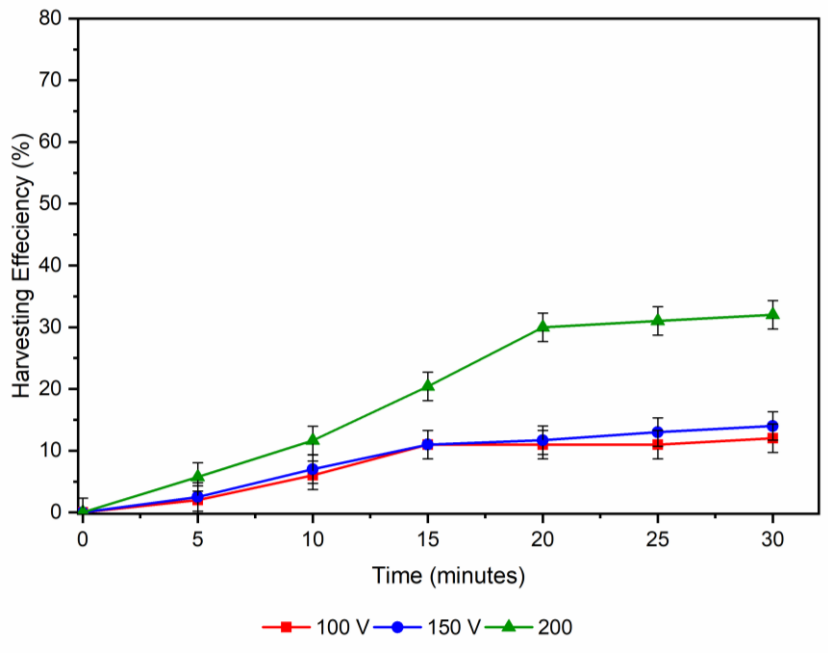

Figure 15. the effect of applied voltages on the harvesting efficiency at frequenscy of 250 kHz and interelectrode distance of 8 mm.

4.3 Effect of Interelectrode Distance on Harvesting Efficiency

The effect of interelectrode distance on the DEP force field represented as the squared electric field $|\nabla E^2|$ was numerically evaluated. Then, the effect of interelectrode distance on microalgae harvesting efficiency at a range of application times was experimented. The studied interelectrode distances were: 4 mm, 6 mm, and 8 mm, and the applied voltage and frequency were kept constant at 200 V and 250 kHz, respectively. **Error! Reference source not found.**16 shows the DEP force field d istribution, and the intensity of the DEP force field increased with decreasing the interelectrode distance form 8 mm, 6 mm, to 4 mm. In Figure 17, the calculated value of the DEP force represented by the square of the electric field ($\nabla|E|^2$) was shown. The maximum squared electric field intensities were 1.26×10^{13}, 7.58×10^{12}, and 5.37×10^{12} V^2/m^3 for an interelectrode distance of 4, 6 and 8 mm, respectively. Moreover, for 4, 6 and 8 mm interelectrode distances, the minimum squared electric field intensity was observed at a distance of 0.314, 0.374 and 0.239 mm, respectively,

from the surface of the electrode. This implies that, increasing the interelectrode distance would result in large areas without any DEP force field, thus lower harvesting efficiency. From Figure 16 and Figure 17, it can be stated that stronger DEP force field is present on the electrode surface and increased with using smaller interelectrode distance, and that higher harvesting efficiency of microalgae could be obtained at lower interelectrode distance. The experimental results in Figure 18a showed that with using an interelectrode distance of 6 and 8 mm and 200 V, the harvesting efficiency increased with time reaching up to 63.9% and 30%, respectively, after 30 minutes of electric field application. This is due to the stronger DEP force exerted on the microalgae cells with smaller interelectrode distance as predicted by the numerical simulation. However, at a smaller interelectrode distance of 4 mm and after a longer time of electric field application the harvesting efficiency of microalgae started to decrease drastically. It was found that the harvesting efficiency of microalgae decreased 70% at 20 minutes to 26.5% at 30 minutes. This finding is opposite to the results predicted by the numerical simulation, where at a smaller interelectrode distance of 4 mm higher harvesting efficiency is expected. The decrease of the harvesting efficiency of the microalgae at an interelectrode distance of 4 mm and after 20 minutes of application time is due to the joule heating effect. At a lower interelectrode distance (i.e., 4 mm), a short circuit occurred due to the formation of pearl-chain of microalgae cells. These pearl-chains might potentially bridge the two electrodes with each other which would generate a short circuit that will increase the electric field intensity (Y. Wang et al., 2014). Such high electric field intensity is associated with increase in medium temperature and induce joule heating effect (Sridharan et al., 2011). As shown in Figure 18b, the strong electric field at an interelectrode distance of 4 mm resulted in increase in temperature from

21 °C to 63.4 °C after 30 minutes. The high temperature resulted in the formation of water bubbles close to the surface of the electrodes which disrupted the harvesting process and started breaking down and dispersing the already entrapped microalgae agglomerates (Yan et al., 2017). The effect of interelectrode distances on the harvesting efficiency of microalgae at 150 V and 100 V is shown in Figure 24 and Figure 25 in the appendix, respectively.

The formation of pearl-chains of microalgae cells is shown in Figure 19, with application of high voltage of 200 V and using small interelectrode distance of 4 mm. At first, the microalgae cells accumulated and entrapped efficiently between the two electrodes due to the polarization of the cells and the presence of strong electric field. Other microalgae cells started to accumulate on the surface of the electrode and form chains of microalgae cells as shown in Figure 19e. After few minutes, the temperature of the medium started to increase due to the strong electric field and generate joule heating effect. The joule heating effect in the reactor induce electrothermal fluid flow, and air bubbles started to form as shown in Figure 19i. Consequently, the pearl chains were broken thus disturbing the harvesting of microalgae. It is important to mention that the pearl chain phenomena will only occur when provided a strong enough voltage amplitude. If weak voltage amplitude is applied, short chains of microalgae cells are formed which will not reach the opposite electrode to form DEP bridge regardless of the concentration of algal cells.

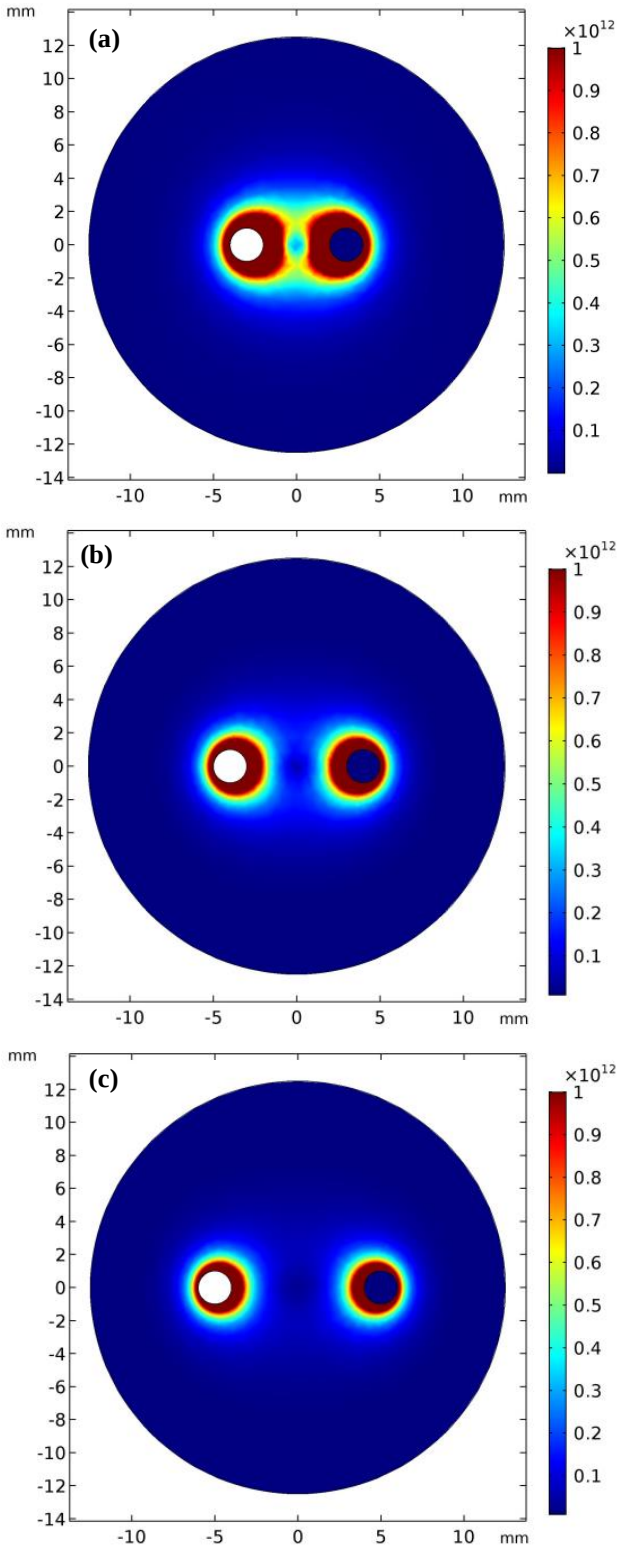

Figure 16. The DEP force field distribution defined as ($\nabla|E|^2$) for interelectrode distances of (a) 4 mm (b) 6 mm and (c) 8 mm at an applied voltage of 200 V and frequency of 250 kHz.

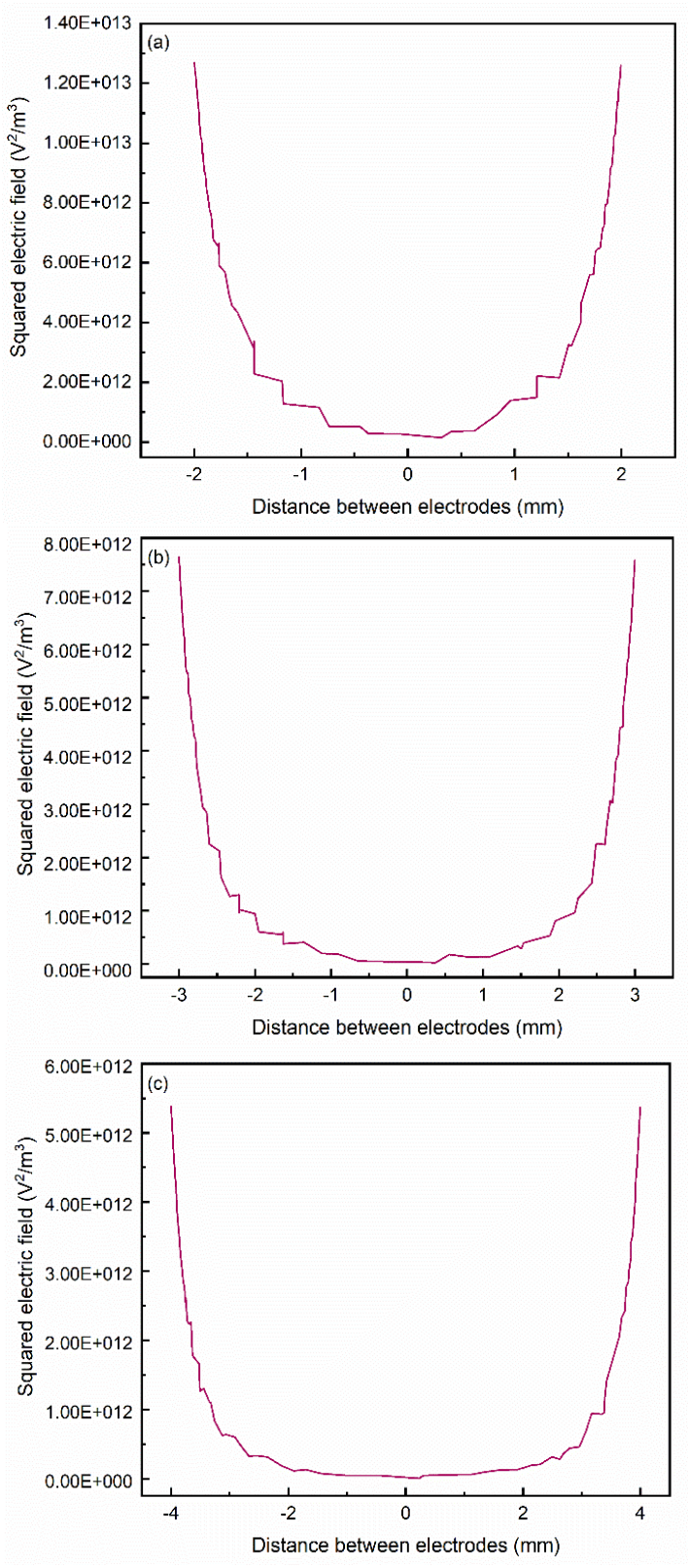

Figure 17. The calculated DEP force field defined as ($\nabla|E|^2$) for interelectrode distances of (a) 4 mm (b) 6 mm and (c) 8 mm at an applied voltage of 200 V and frequency of 250 kHz.

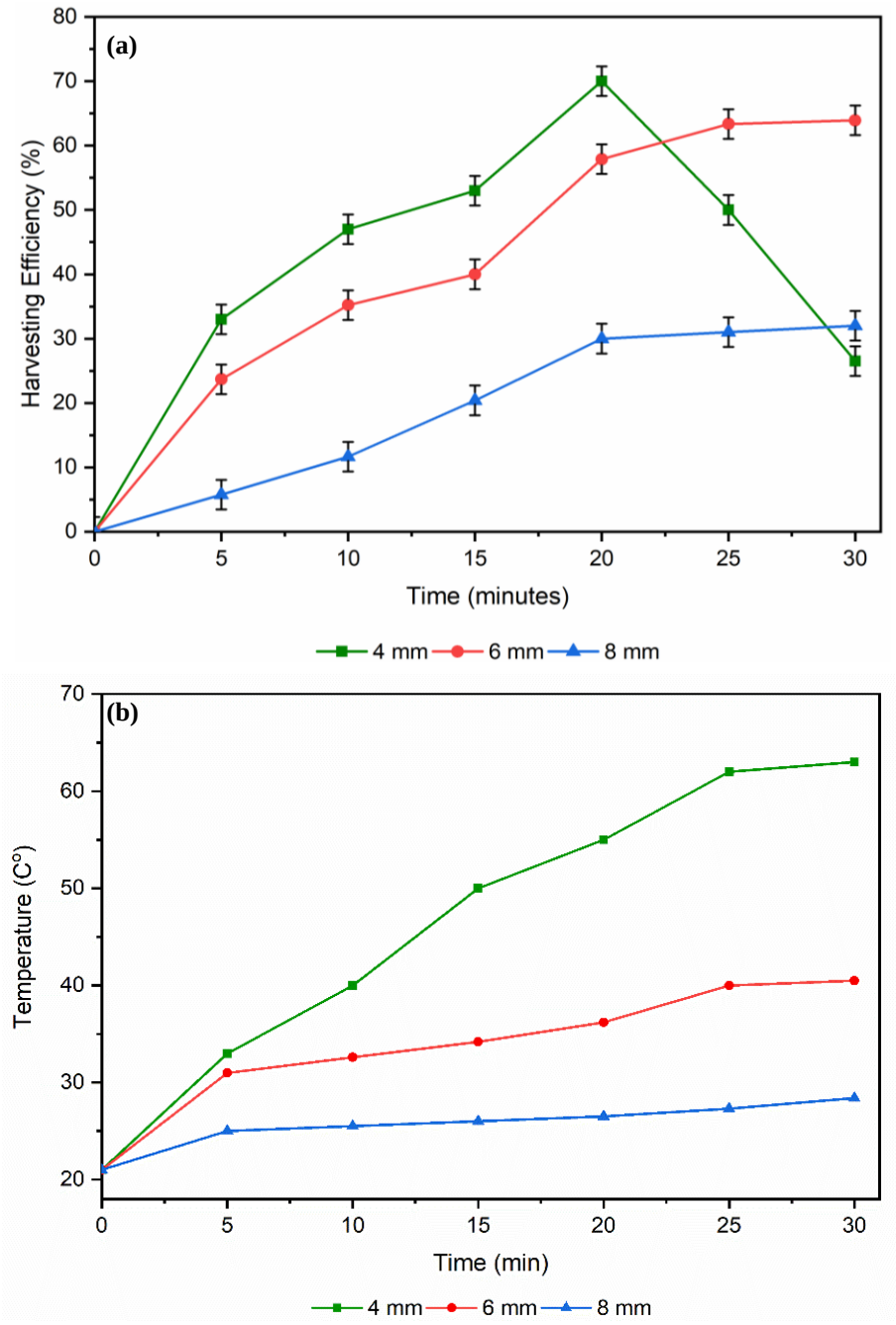

Figure 18. (a) effect of inter-electrode distance on the harvesting efficiency using 200 V and 250 kHz, (b) temperature increase at the same conditions due to joule heating effect.

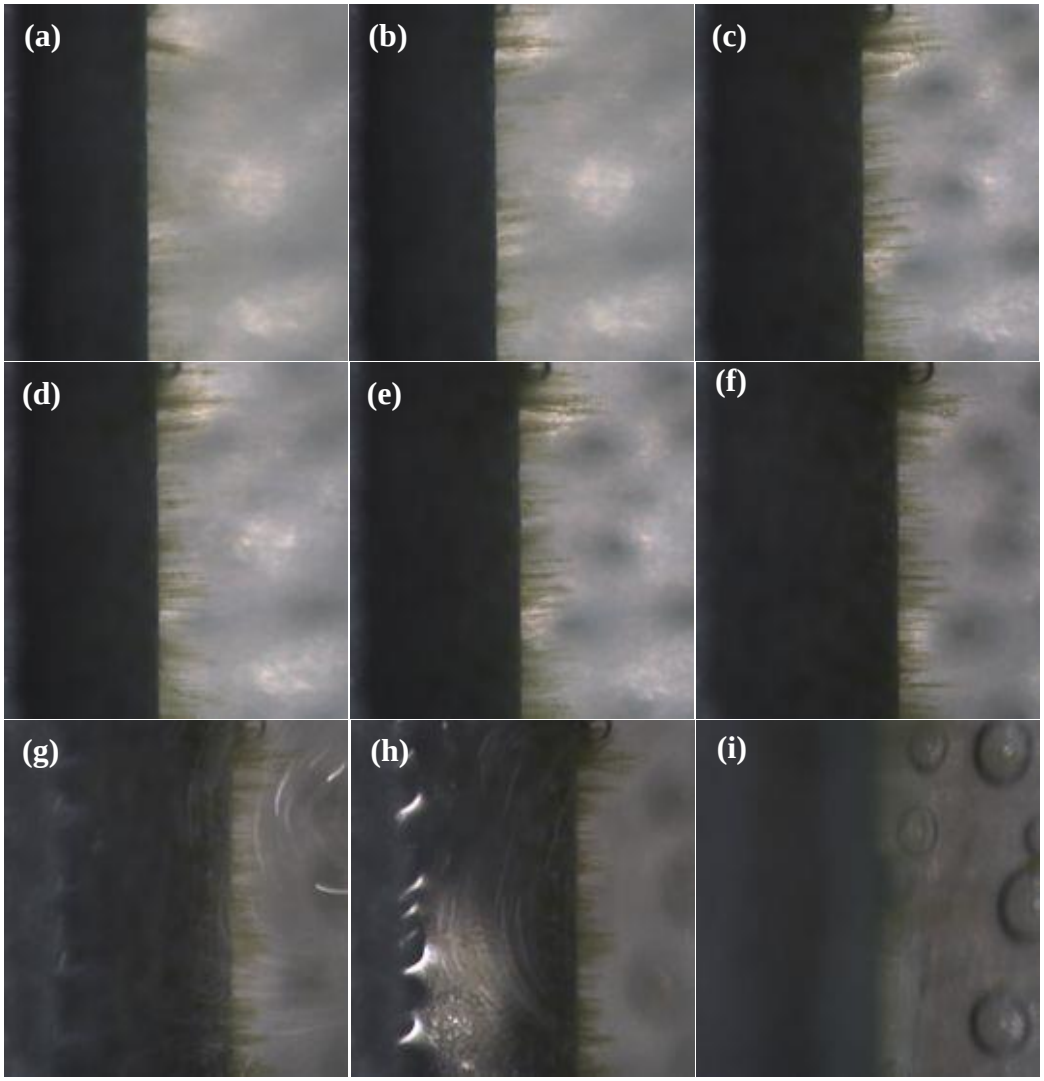

Figure 19. The formation of pearl-chain effect, and the disturbance of the chains due to electrothermal fluid flow induced by joule heating effect.

4.4 Effect of Pulsed Electric Field on Harvesting Efficiency

Due to the solution temperature increase which was accompanied by the small interelectrode distance (i.e., 4 mm) and longer time of continuous electric field application (more than 20 minutes), the harvesting efficiency using a pulsed electric field was investigated. A pulsed electric field of 2 minutes ON and 2 minutes OFF for 10, 20, and 30 minutes at interelectrode distances of 4 mm and 6 mm was investigated. The applied voltage and frequency were kept constant at 200 V and 250 kHz, respectively. Figure 20a shows that at an interelectrode distance of 4 mm the

harvesting efficiency was 76.6% and 26.5% after 30 minutes for pulsed electric field and continuous electric field, respectively. The harvesting efficiency of microalgae using a pulsed electric was 50% higher than that of continuous electric field after 30 minutes. It was observed that when the electric field was ON, the microalgae was entrapped between the two electrodes as mentioned earlier and when the electric field was turned OFF the formed large agglomerates settled down due to the gravitational force. Furthermore, the negative effect of joule heating and disturbance of the harvesting process due to increase of temperature did not occur in the pulsed electric filed. The highest temperature measured after 30 minutes was 63 ^{o}C and 46 ^{o}C for continuous and pulsed electric field, respectively. At an interelectrode distance of 6 mm it was observed that the temperature of solution did not increase significantly in the continuous and pulsed electric field application. The highest temperature after 30 minutes of electric field application was 44^{o}C and 40^{o}C for continuous and pulsed electric field, respectively. Due to the longer time of electric field application using the continuous electric field, the harvesting efficiency of microalgae was higher than the pulsed electric field at 6 mm electrode distance. With the continuous electric field, the harvesting efficiency was 63.9% compared to 42.8% for the pulsed electric field after 30 minutes (Figure 20b). This signifies the advantage of using pulsed electric field over continuous electric field for small interelectrode distances where the harvesting efficiency is high, and the expected energy consumption is low. The energy requirements are discussed later.

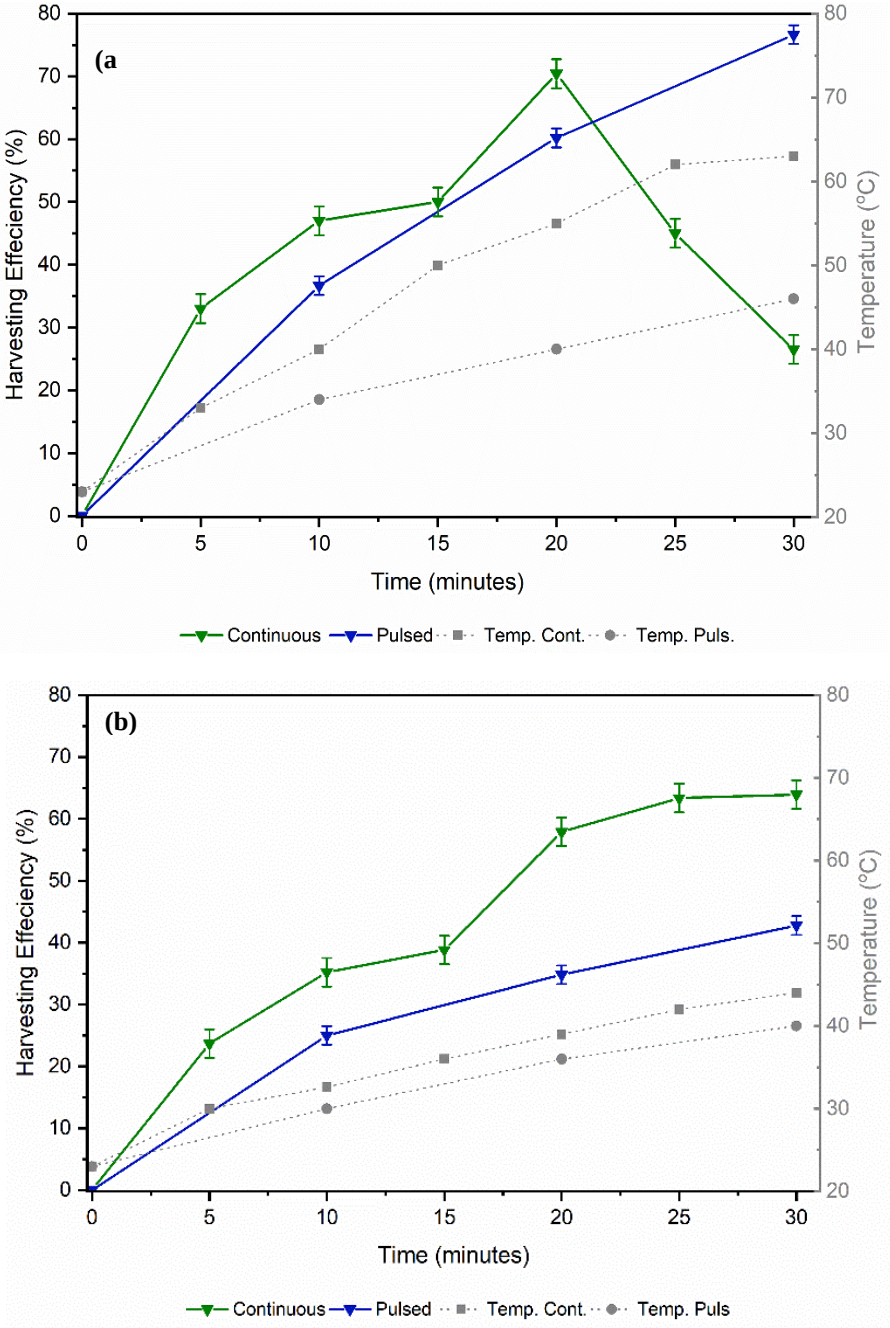

Figure 20. Effect of pulsed electric field on the microalgae harvesting efficiency at voltage 200 V, frequency 250 kHz, and interelectrode distance of (a) 4 mm and (b) 6 mm.

4.5 Effect of AC Frequency on Harvesting Efficiency

The effect of the applied current frequency on the microalgae harvesting efficiency was evaluated at a low frequency of 50 Hz and four high frequencies: 100 kHz, 150 kHz, 200 kHz and 250 kHz. The applied voltage, the experimental time,

and the interelectrode distance were kept constant at 200 V, 20 minutes, and 6 mm, respectively. As shown in Figure 21, the harvesting efficiencies of microalgae were 20%, 67%, and 57.9%, at frequency of 50 Hz, 100-150 kHz, and 200-250 kHz, respectively. At low frequency, the DEP response of the cell depends on the conductivities of the cell and the medium. The low conductivity of the cell wall and membrane compared to the conductivity of the medium result in nDEP behavior, hence low harvesting efficiency of microalgae cells (Gallo-Villanueva et al., 2011). At an intermediate frequency of 100-150 kHz, the DEP behavior is dominated by the conductivity of cell cytoplasm. The microalgae cell cytoplasm has higher conductivity than the medium, therefore it is more polarizable than the medium resulting in pDEP behavior. Hence the harvesting efficiency of microalgae cells increase at intermediate frequencies. At higher frequencies of 200-250 kHz, the DEP response of the cell is dominated by the permittivity of the cell and the medium. Due to the low permittivity of microalgae cell cytoplasm and high permittivity of the medium, microalgae cells show nDEP behavior (Fernandez et al., 2017). Hence, low harvesting efficiencies at higher frequencies of 200 kHz and 250 kHz.

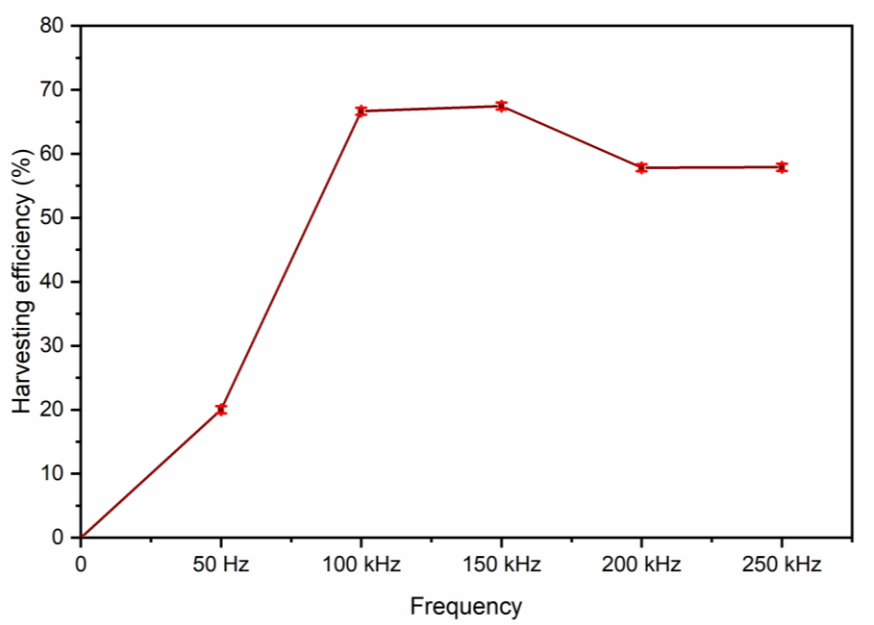

Figure 21. Effect of the applied AC frequency on the harvesting efficiency of microalgae using an applied voltage of 200 V, and interelectrode distance of 6 mm after 20 minutes.

4.6 Specific Energy Consumption

This section studies the effect of applied voltage and interelectrode distance on the specific energy consumption. As shown in Figure 22a, the specific energy consumption at small interelectrode distance of 4 mm decreased as the applied voltage increased. However, at larger interelectrode distances of 6 and 8 mm, the specific energy consumption increased as the applied voltage increased. At small interelectrode distance, the specific energy consumption decreased as the applied voltage increased due to the significant improvement in the harvesting efficiency. While using large interelectrode distance, the specific energy consumption increased as the applied voltage increased due to the minimal improvement in the harvesting efficiency although higher voltage has been used. As shown in Figure 22b, the specific energy consumption using pulsed electrical field was less than the continuous mode. At an applied voltage of 200 V and interelectrode distance of 4 mm, the

specific energy consumption of pulsed mode was 70% lower than the continuous mode. While using the same applied voltage and interelectrode distance of 6 mm, the specific energy consumption of pulsed mode was 38% lower than the continuous mode. The specific energy consumption of the pulsed mode was lower since the electric field was applied for half the time of the continuous mode.

To find the most optimum operating conditions, the specific energy consumption and harvesting efficiency were normalized using Equation 5. As shown in Figure 23, the most efficient running conditions were: (1) pulsed electric field at small interelectrode distance and high applied voltage, (2) continuous electric field at small interelectrode distance and mid applied voltage, (3) continuous electric field at mid interelectrode distance and high applied voltage. The most efficient running conditions had an energy consumption of 7.76 kWh/kg with harvesting efficiency of 76.6%. On the other hand, the least efficient running conditions was obtained using continuous electric field at large interelectrode distance and mid/low applied voltage. The specific energy consumption of the least efficient running conditions (continuous electric field at 4 mm, 200 V, and 30 minutes) was 26.4 kWh/kg with harvesting efficiency of 26.5%.

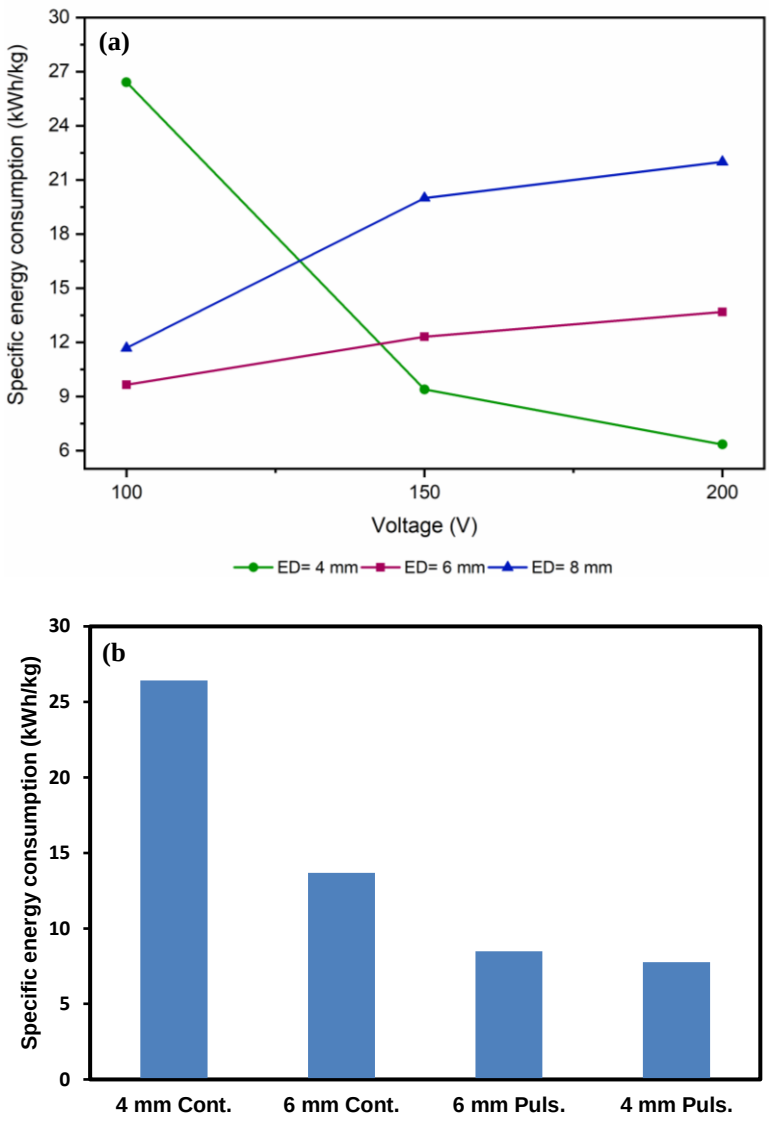

Figure 22. Specific energy consumption for various experimental conditions used in this study. (a) continuous application of electric field at 100, 150, and 200 V, and 4, 6, and 8 mm. (b) continuous and pulsed electric field at 4 and 6 mm, 200 V, for 30 minutes.

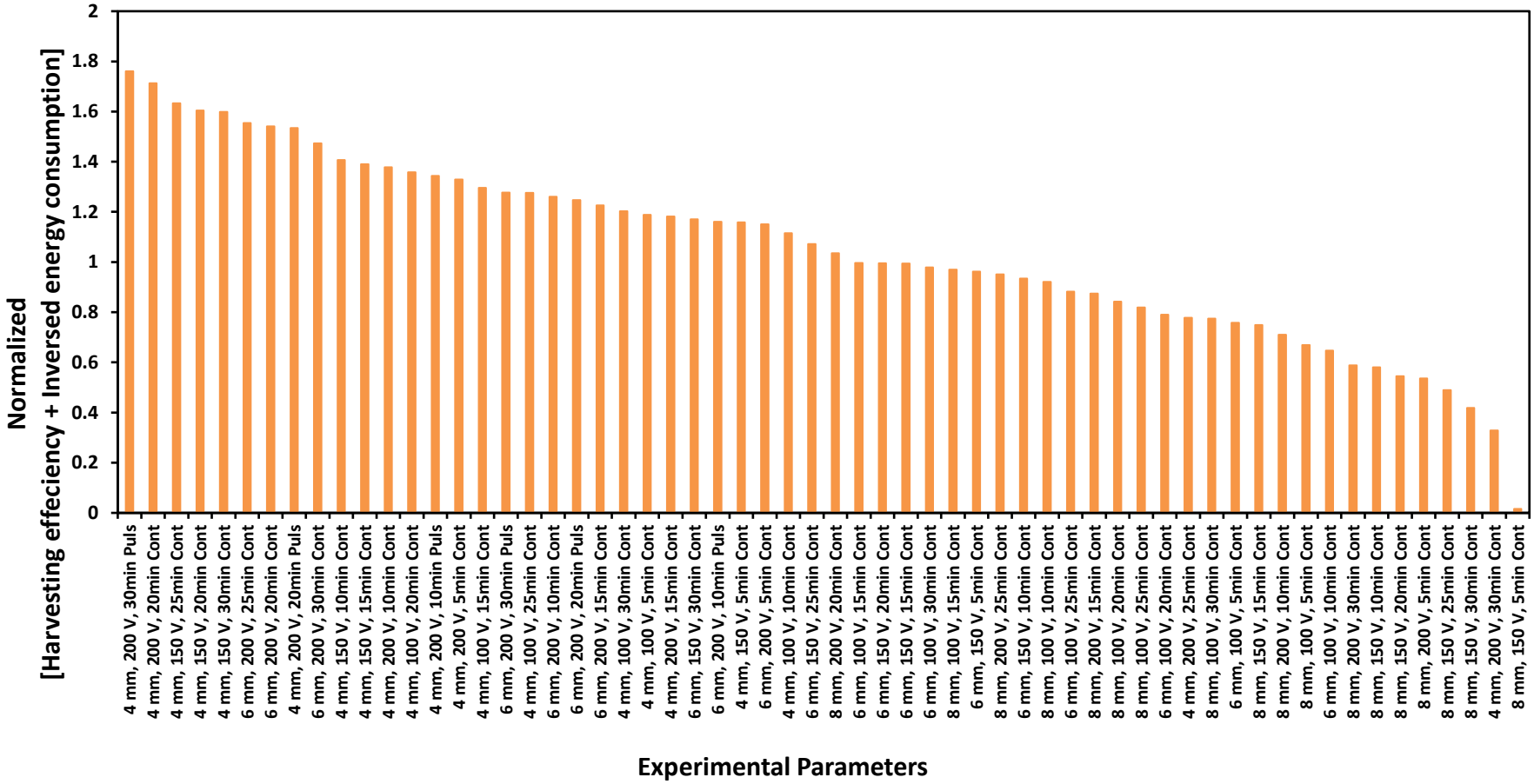

Figure 23. The normalized harvesting efficiency and inversed energy consumption of various experimental conditions used in this study.

Chapter 5: Conclusion

In this study, a novel titanium dioxide insulated stainless steel electrode has been used for the harvesting of *Chlorella sp.* microalgae from freshwater by dielectrophoretic force. An interdigitated electrodes configuration was used to increase the inhomogeneity of the AC electric field. The batch reactor used was in the range of 50 milliliters. The major enhancement of using the new electrode configuration was achieving high harvesting efficiency with zero metal contamination for the harvested biomass due to electrodes insulation. The effect of interelectrode distance and applied voltage on the intensity of DEP force was stimulated. For the simulation studies, it was found that DEP force was intensified with higher applied voltage and smaller interelectrode distance. The effect of several experimental parameters on the harvesting efficiency of microalgae was investigated. It was found that the highest harvesting efficiency of microalgae achieved was 76.6% with energy consumption of 7.76 kWh/kg, obtained with application of pulsed electric field at 4 mm interelectrode distance, 250 kHz frequency, and 200 V applied voltage for 30 minutes. The decrease in harvesting efficiency with application of strong electric field due to joule heating effect was reduced with application of pulsed DEP. The most significant impact of using the new electrode configuration is achieving high harvesting efficiency with no contamination for the harvested biomass. Future studies to enhance DEP technology could focus on the impact of DEP on microalgae groups other than green microalgae, in addition to investigate the manipulation and separation of multiple microalgae cells spontaneously. Also, separation of microalgae in continuous flow and larger scales, and to experiment with regular culture mediums.

References

Abt, V., Gringel, F., Han, A., Neubauer, P., & Birkholz, M. (2020). Separation, characterization, and handling of microalgae by dielectrophoresis. In *Microorganisms* (Vol. 8, Issue 4, pp. 1–19). https://doi.org/10.3390/microorganisms8040540

Adarme-Vega, T. C., Lim, D. K. Y., Timmins, M., Vernen, F., Li, Y., & Schenk, P. M. (2012). Microalgal biofactories: a promising approach towards sustainable omega-3 fatty acid production. In *Microbial Cell Factories* (Vol. 11, Issue 1, pp. 1–10). BioMed Central. https://doi.org/10.1186/1475-2859-11-96

Ahmad, A. L., Mat Yasin, N. H., Derek, C. J. C., & Lim, J. K. (2011). Optimization of microalgae coagulation process using chitosan. *Chemical Engineering Journal*, *173*(3), 879–882. https://doi.org/10.1016/j.cej.2011.07.070

Alkhatib, A. M., Hawari, A. H., Ammar, M., & Benamor, A. (2020). A novel cylindrical electrode configuration for inducing dielectrophoretic forces during electrocoagulation. *Journal of Water Process Engineering*, *35*(February). https://doi.org/10.1016/j.jwpe.2020.101195

Alnaimat, F., Mathew, B., & Hilal-Alnaqbi, A. (2020). Modeling a dielectrophoretic microfluidic device with vertical interdigitated transducer electrodes for separation of microparticles based on size. *Micromachines*, *11*(6). https://doi.org/10.3390/MI11060563

Bahi, M. M., Tsaloglou, M. N., Mowlem, M., & Morgan, H. (2011). Electroporation and lysis of marine microalga Karenia brevis for RNA extraction and amplification. *Journal of the Royal Society Interface*, *8*(57), 601–608. https://doi.org/10.1098/rsif.2010.0445

Bakır, M., Dalgaç, Ş., Ünal, E., Karadağ, F., Demirci, M., Köksal, A. S., Akgöl, O., & Karaaslan, M. (2019). High Sensitive Metamaterial Sensor for Water Treatment Centres. *Water, Air, and Soil Pollution*, *230*(12). https://doi.org/10.1007/s11270-019-4355-y

Balasubramanian, A. K., Soni, K. A., Beskok, A., & Pillai, S. D. (2007). A microfluidic device for continuous capture and concentration of microorganisms from potable water. *Lab on a Chip*, *7*(10), 1315–1321. https://doi.org/10.1039/b706559k

Ballantyne, G. R., & Holtham, P. N. (2010). Application of dielectrophoresis for the separation of minerals. *Minerals Engineering*, *23*(4), 350–358. https://doi.org/10.1016/j.mineng.2009.09.001

Barros, A. I., Gonçalves, A. L., Simões, M., & Pires, J. C. M. (2015). Harvesting techniques applied to microalgae: A review. *Renewable and Sustainable Energy Reviews*, *41*, 1489–1500. https://doi.org/10.1016/J.RSER.2014.09.037

Bilad, M. R., Vandamme, D., Foubert, I., Muylaert, K., & Vankelecom, I. F. J. (2012). Harvesting microalgal biomass using submerged microfiltration membranes. *Bioresource Technology*, *111*, 343–352. https://doi.org/10.1016/j.biortech.2012.02.009

Branyikova, I., Prochazkova, G., Potocar, T., Jezkova, Z., & Branyik, T. (2018). Harvesting of microalgae by flocculation. *Fermentation*, *4*(4), 93. https://doi.org/10.3390/fermentation4040093

Brennan, L., & Owende, P. (2010). Biofuels from microalgae-A review of technologies for production, processing, and extractions of biofuels and co-products. *Renewable and Sustainable Energy Reviews*, *14*(2), 557–577.

https://doi.org/10.1016/j.rser.2009.10.009

Buono, S., Langellotti, A. L., Martello, A., Rinna, F., & Fogliano, V. (2014). Functional ingredients from microalgae. *Food & Function*, *5*(8), 1669–1685. https://doi.org/10.1039/C4FO00125G

Calero, V., Garcia-Sanchez, P., Ramos, A., & Morgan, H. (2019). Combining DC and AC electric fields with deterministic lateral displacement for micro- And nano-particle separation. *Biomicrofluidics*, *13*(5), 054110. https://doi.org/10.1063/1.5124475

Carmichael, W. W., Drapeau, C., & Anderson, D. M. (2000). Harvesting of Aphanizomenon flos-aquae Ralfs ex Born. & Flah. var. flos-aquae (Cyanobacteria) from Klamath Lake for human dietary use. *Journal of Applied Phycology*, *12*(6), 585–595. https://doi.org/10.1023/A:1026506713560

Çetin, B., & Li, D. (2011). Dielectrophoresis in microfluidics technology. In *Electrophoresis* (Vol. 32, Issue 18, pp. 2410–2427). https://doi.org/10.1002/elps.201100167

Chen, G. (2004). Electrochemical technologies in wastewater treatment. *Separation and Purification Technology*, *38*(1), 11–41. https://doi.org/10.1016/j.seppur.2003.10.006

Chen, Y. M., Liu, J. C., & Ju, Y. H. (1998). Flotation removal of algae from water. *Colloids and Surfaces B: Biointerfaces*, *12*(1), 49–55. https://doi.org/10.1016/S0927-7765(98)00059-9

Cheruvu, S., Van Ginkel, S., Wei, X., Zhang, X., Steiner, D., Rego De Oliveira, S. H., Xu, C., Kalil Duarte, L. H., Salvi, E., Hu, Z., Lee, H. J., Gijon-Felix, R., & Chen,

Y. (2016). Algae harvesting. *Membrane Technologies for Biorefining*, 309–328. https://doi.org/10.1016/B978-0-08-100451-7.00013-X

Christenson, L., & Sims, R. (2011). Production and harvesting of microalgae for wastewater treatment, biofuels, and bioproducts. In *Biotechnology Advances* (Vol. 29, Issue 6, pp. 686–702). Elsevier. https://doi.org/10.1016/j.biotechadv.2011.05.015

Dassey, A. J., & Theegala, C. S. (2013). Harvesting economics and strategies using centrifugation for cost effective separation of microalgae cells for biodiesel applications. *Bioresource Technology*, *128*, 241–245. https://doi.org/10.1016/j.biortech.2012.10.061

Dineshbabu, G., Goswami, G., Kumar, R., Sinha, A., & Das, D. (2019). Microalgae–nutritious, sustainable aqua- and animal feed source. *Journal of Functional Foods*, *62*, 103545. https://doi.org/10.1016/j.jff.2019.103545

Drexler, I. L. C., & Yeh, D. H. (2014). Membrane applications for microalgae cultivation and harvesting: a review. *Reviews in Environmental Science and Biotechnology*, *13*(4), 487–504. https://doi.org/10.1007/s11157-014-9350-6

Du, F., Hawari, A., Baune, M., & Thöming, J. (2009). Dielectrophoretically intensified cross-flow membrane filtration. *Journal of Membrane Science*, *336*(336), 71–78. https://doi.org/10.1016/j.memsci.2009.03.010

Du, F, Ciaciuch, P., Bohlen, S., Wang, Y., Baune, M., & Thöming, J. (2013). Intensification of cross-flow membrane filtration using dielectrophoresis with a novel electrode configuration. *Journal of Membrane Science*, *448*, 256–261. https://doi.org/10.1016/j.memsci.2013.08.016

Du, Fei, Hawari, A. H., Larbi, B., Ltaief, A., Pesch, G. R., Baune, M., & Thöming, J. (2018). Fouling suppression in submerged membrane bioreactors by obstacle dielectrophoresis. *Journal of Membrane Science*, *549*(October 2017), 466–473. https://doi.org/10.1016/j.memsci.2017.12.049

Edzwald, J. K. (1993). Algae, bubbles, coagulants, and dissolved air flotation. *Water Science and Technology*, *27*(10), 67–81. https://doi.org/10.2166/wst.1993.0207

Ensano, B. M. B., Borea, L., Naddeo, V., Belgiorno, V., de Luna, M. D. G., & Ballesteros, F. C. (2016). Combination of electrochemical processes with membrane bioreactors for wastewater treatment and fouling Control: A review. *Frontiers in Environmental Science*, *4*(AUG). https://doi.org/10.3389/fenvs.2016.00057

Fayad, N., Yehya, T., Audonnet, F., & Vial, C. (2017). Harvesting of microalgae Chlorella vulgaris using electro-coagulation-flocculation in the batch mode. *Algal Research*, *25*, 1–11. https://doi.org/10.1016/j.algal.2017.03.015

Fernandez, R. E., Rohani, A., Farmehini, V., & Swami, N. S. (2017). Review: Microbial analysis in dielectrophoretic microfluidic systems. *Analytica Chimica Acta*, *966*, 11–33. https://doi.org/10.1016/j.aca.2017.02.024

Figueroa, M., Vázquez-Padín, J. R., Mosquera-Corral, A., Campos, J. L., & Méndez, R. (2012). Is the CANON reactor an alternative for nitrogen removal from pre-treated swine slurry? *Biochemical Engineering Journal*, *65*, 23–29. https://doi.org/10.1016/j.bej.2012.03.008

Fox, J. M., & Zimba, P. V. (2018). Minerals and trace elements in microalgae. In *Microalgae in Health and Disease Prevention* (pp. 177–193). Academic Press. https://doi.org/10.1016/B978-0-12-811405-6.00008-6

Gallo-Villanueva, R. C., Jesús-Pérez, N. M., Martínez-López, J. I., Pacheco, A., & Lapizco-Encinas, B. H. (2011). Assessment of microalgae viability employing insulator-based dielectrophoresis. *Microfluidics and Nanofluidics*, *10*(6), 1305–1315. https://doi.org/10.1007/s10404-010-0764-3

Gao, S., Yang, J., Tian, J., Ma, F., Tu, G., & Du, M. (2010). Electro-coagulation-flotation process for algae removal. *Journal of Hazardous Materials*, *177*(1–3), 336–343. https://doi.org/10.1016/j.jhazmat.2009.12.037

Garg, S., Li, Y., Wang, L., & Schenk, P. M. (2012). Flotation of marine microalgae: Effect of algal hydrophobicity. *Bioresource Technology*, *121*, 471–474. https://doi.org/10.1016/j.biortech.2012.06.111

Giesler, J., Pesch, G. R., Weirauch, L., Schmidt, M. P., Thöming, J., & Baune, M. (2020). Polarizability-dependent sorting of microparticles using continuous-flow dielectrophoretic chromatography with a frequency modulation method. *Micromachines*, *11*(1), 1–14. https://doi.org/10.3390/mi11010038

Goldemberg, J. (2007). Ethanol for a sustainable energy future. *Science*, *315*(5813), 808–810. https://doi.org/10.1126/science.1137013

Gouveia, L., Oliveira, A. C., Congestri, R., Bruno, L., Soares, A. T., Menezes, R. S., Filho, N. R. A., & Tzovenis, I. (2017). Biodiesel from microalgae. In *Microalgae-Based Biofuels and Bioproducts: From Feedstock Cultivation to End-Products*. Elsevier Ltd. https://doi.org/10.1016/B978-0-08-101023-5.00010-8

Hadady, H., Redelman, D., Hiibel, S. R., & Geiger, E. J. (2016). Continuous-flow sorting of microalgae cells based on lipid content by high frequency dielectrophoresis. *AIMS Biophysics*, *3*(3), 398–414.

https://doi.org/10.3934/biophy.2016.3.398

Hanotu, J., Bandulasena, H. C. C. H., & Zimmerman, W. B. (2012). Microflotation performance for algal separation. *Biotechnology and Bioengineering*, *109*(7), 1663–1673. https://doi.org/10.1002/bit.24449

Hashim, M. A., Mukhopadhyay, S., Sahu, J. N., & Sengupta, B. (2011). Remediation technologies for heavy metal contaminated groundwater. In *Journal of Environmental Management* (Vol. 92, Issue 10, pp. 2355–2388). Academic Press. https://doi.org/10.1016/j.jenvman.2011.06.009

Hawari, A. H., Alkhatib, A. M., Das, P., Thaher, M., & Benamor, A. (2020). Effect of the induced dielectrophoretic force on harvesting of marine microalgae (Tetraselmis sp.) in electrocoagulation. *Journal of Environmental Management*, *260*(January), 110106. https://doi.org/10.1016/j.jenvman.2020.110106

Hawari, A. H., Alkhatib, A. M., Hafiz, M., & Das, P. (2020). A novel electrocoagulation electrode configuration for the removal of total organic carbon from primary treated municipal wastewater. *Environmental Science and Pollution Research*, 23888–23898. https://doi.org/https://doi.org/10.1007/s11356-020-08678-4

Hawari, A. H., Du, F., Baune, M., & Thöming, J. (2015). A fouling suppression system in submerged membrane bioreactors using dielectrophoretic forces. *Journal of Environmental Sciences (China)*, *29*, 139–145. https://doi.org/10.1016/j.jes.2014.07.027

Hawari, A., Larbi, B., Alkhatib, A., Du, F., Baune, M., & Thöming, J. (2019). Insulator-based dielectrophoresis for fouling suppression in submerged membranes bioreactors: Impact of insulators shape and dimensions. *Separation*

and Purification Technology, *213*(September 2018), 507–514. https://doi.org/10.1016/j.seppur.2018.12.084

Hawari, A., Larbi, B., Alkhatib, A., Yasir, A., Du, F., Baune, M., & Thöming, J. (2019). Impact of aeration rate and dielectrophoretic force on fouling suppression in submerged membrane bioreactors. *Chemical Engineering & Processing*, *142*(June). https://doi.org/10.1016/j.cep.2019.107565

Hawkins, B. G., Lai, N., & Clague, D. S. (2020). High-sensitivity in dielectrophoresis separations. *Micromachines*, *11*(4). https://doi.org/10.3390/MI11040391

Henderson, R. K., Parsons, S. A., & Jefferson, B. (2010). The impact of differing cell and algogenic organic matter (AOM) characteristics on the coagulation and flotation of algae. *Water Research*, *44*(12), 3617–3624. https://doi.org/10.1016/j.watres.2010.04.016

Honegger, T., Berton, K., Picard, E., & Peyrade, D. (2011). Determination of Clausius-Mossotti factors and surface capacitances for colloidal particles. *Applied Physics Letters*, *98*(18), 2011–2014. https://doi.org/10.1063/1.3583441

Hughes, M. P. (2016). Fifty years of dielectrophoretic cell separation technology. *Biomicrofluidics*, *10*(3), 032801. https://doi.org/10.1063/1.4954841

Jakoby, B., & Vellekoop, M. J. (2004). Physical sensors for water-in-oil emulsions. *Sensors and Actuators, A: Physical*, *110*(1–3), 28–32. https://doi.org/10.1016/j.sna.2003.08.005

Jarvis, P., Buckingham, P., Holden, B., & Jefferson, B. (2009). Low energy ballasted flotation. *Water Research*, *43*(14), 3427–3434. https://doi.org/10.1016/j.watres.2009.05.003

Jegannathan, K. R., Chan, E. S., & Ravindra, P. (2009). Harnessing biofuels: A global Renaissance in energy production? *Renewable and Sustainable Energy Reviews*, *13*(8), 2163–2168. https://doi.org/10.1016/J.RSER.2009.01.012

Jesús-Pérez, N. M., & Lapizco-Encinas, B. H. (2011). Dielectrophoretic monitoring of microorganisms in environmental applications. *Electrophoresis*, *32*(17), 2331–2357. https://doi.org/10.1002/elps.201100107

Jones, E. R., Van Vliet, M. T. H., Qadir, M., & Bierkens, M. F. P. (2021). Country-level and gridded estimates of wastewater production, collection, treatment and reuse. *Earth System Science Data*, *13*(2), 237–254. https://doi.org/10.5194/essd-13-237-2021

Jubery, T. Z., Srivastava, S. K., & Dutta, P. (2014). Dielectrophoretic separation of bioparticles in microdevices: A review. *Electrophoresis*, *35*(5), 691–713. https://doi.org/10.1002/elps.201300424

Kalantar-Zadeh, K., Khoshmanesh, K., Kayani, A. A., Nahavandi, S., & Mitchell, A. (2010). Dielectrophoretically tuneable optical waveguides using nanoparticles in microfluidics. *Applied Physics Letters*, *96*(10), 101108. https://doi.org/10.1063/1.3358384

Khan, M. I., Shin, J. H., & Kim, J. D. (2018). The promising future of microalgae: Current status, challenges, and optimization of a sustainable and renewable industry for biofuels, feed, and other products. *Microbial Cell Factories*, *17*(1), 1–21. https://doi.org/10.1186/s12934-018-0879-x

Khatib, W. A., Ayari, A., Yasir, A. T., Talhami, M., Das, P., Quadir, M. A., & Hawari, A. H. (2021). Enhancing the electrocoagulation process for harvesting marine microalgae (Tetraselmis sp.) using interdigitated electrodes. *Journal of*

Environmental Management, *292*. https://doi.org/10.1016/j.jenvman.2021.112761

Khoo, K. S., Chew, K. W., Yew, G. Y., Leong, W. H., Chai, Y. H., Show, P. L., & Chen, W. H. (2020). Recent advances in downstream processing of microalgae lipid recovery for biofuel production. In *Bioresource Technology* (Vol. 304, p. 122996). Elsevier Ltd. https://doi.org/10.1016/j.biortech.2020.122996

Khoshmanesh, K., Nahavandi, S., Baratchi, S., Mitchell, A., & Kalantar-zadeh, K. (2011). Dielectrophoretic platforms for bio-microfluidic systems. In *Biosensors and Bioelectronics* (Vol. 26, Issue 5, pp. 1800–1814). Elsevier. https://doi.org/10.1016/j.bios.2010.09.022

Kim, D., Sonker, M., & Ros, A. (2019). Dielectrophoresis: From Molecular to Micrometer-Scale Analytes. *Analytical Chemistry*, *91*(1), 277–295. https://doi.org/10.1021/acs.analchem.8b05454

Kim, J., Ryu, B. G., Kim, B. K., Han, J. I., & Yang, J. W. (2012). Continuous microalgae recovery using electrolysis with polarity exchange. *Bioresource Technology*, *111*, 268–275. https://doi.org/10.1016/j.biortech.2012.01.104

Kumar, R. T. K., Kanchustambham, P., Kinnamon, D., & Prasad, S. (2017). 2D dielectrophoretic signature of Coscinodiscus wailesii algae in non-uniform electric fields. *Algal Research*, *27*, 109–114. https://doi.org/10.1016/j.algal.2017.08.031

Laamanen, C. A., Ross, G. M., & Scott, J. A. (2016). Flotation harvesting of microalgae. *Renewable and Sustainable Energy Reviews*, *58*, 75–86. https://doi.org/10.1016/J.RSER.2015.12.293

LaLonde, A., Gencoglu, A., Romero-Creel, M. F., Koppula, K. S., & Lapizco-Encinas, B. H. (2014). Effect of insulating posts geometry on particle manipulation in insulator based dielectrophoretic devices. *Journal of Chromatography A*, *1344*, 99–108. https://doi.org/10.1016/j.chroma.2014.03.083

Lalonde, A., Romero-Creel, M. F., & Lapizco-Encinas, B. H. (2015). Assessment of cell viability after manipulation with insulator-based dielectrophoresis. *Electrophoresis*, *36*(13), 1479–1484. https://doi.org/10.1002/elps.201400331

Lapizco-Encinas, B. H. (2018). On the recent developments of insulator-based dielectrophoresis : A review. *Electrophoresis*, *40*, 358–375. https://doi.org/10.1002/elps.201800285

Lapizco-Encinas, B. H., Davalos, R. V., Simmons, B. A., Cummings, E. B., & Fintschenko, Y. (2005). An insulator-based (electrodeless) dielectrophoretic concentrator for microbes in water. *Journal of Microbiological Methods*, *62*(3 SPEC. ISS.), 317–326. https://doi.org/10.1016/j.mimet.2005.04.027

Lapizco-Encinas, B. H., Simmons, B. A., Cummings, E. B., & Fintschenko, Y. (2004a). Dielectrophoretic Concentration and Separation of Live and Dead Bacteria in an Array of Insulators. *Analytical Chemistry*, *76*(6), 1571–1579. https://doi.org/10.1021/ac034804j

Lapizco-Encinas, B. H., Simmons, B. A., Cummings, E. B., & Fintschenko, Y. (2004b). Insulator-based dielectrophoresis for the selective concentration and separation of live bacteria in water. *Electrophoresis*, *25*(10–11), 1695–1704. https://doi.org/10.1002/elps.200405899

Larbi, B., Du, F., Baune, M., Thöming, J., & Hawari, A. (2018). Numerical study on the effect of insulator size and shape on fouling suppression by electrodeless

dielectrophoresis in submerged membrane bioreactors. *Biomicrofluidics*, *1982*. https://doi.org/10.1063/1.5045444

Larbi, B., Hawari, A., Du, F., & Baune, M. (2017). Numerical Simulation of the Electric Field Gradient Squared in a New Electrode Configuration for Fouling Suppression in Submerged Membrane Bioreactors. *ESTEEM Academic Journal*, *13*(2), 18–29.

Larbi, B., Hawari, A., Du, F., Baune, M., & Thöming, J. (2017). Impact of the pulsed voltage input and the electrode spacing on the enhancement of the permeate flux in a dielectrophoresis based anti-fouling system for a submerged membrane bioreactor. *Separation and Purification Technology*, *187*, 102–109. https://doi.org/10.1016/j.seppur.2017.06.045

Larbi, B., Ltaief, A., Hawari, A., Du, F., Baune, M., & Thöming, J. (2017). Assessment of the Effect of Dielectrophoresis (DEP) on the Viability of Activated Sludge Biomass. *International Journal of Environmental Science and Development*, *8*(10), 715–718. https://doi.org/10.18178/ijesd.2017.8.10.1044

Laux, E. M., Bier, F. F., & Hölzel, R. (2018). Electrode-based AC electrokinetics of proteins: A mini-review. In *Bioelectrochemistry* (Vol. 120, pp. 76–82). Elsevier B.V. https://doi.org/10.1016/j.bioelechem.2017.11.010

Lee, A. K., Lewis, D. M., & Ashman, P. J. (2013). Harvesting of marine microalgae by electroflocculation: The energetics, plant design, and economics. *Applied Energy*, *108*, 45–53. https://doi.org/10.1016/j.apenergy.2013.03.003

Lewpiriyawong, N., & Yang, C. (2014). *Dielectrophoresis Field-Flow Fractionation for Continuous-Flow Separation of Particles and Cells in Microfluidic Devices*. 29–62. https://doi.org/10.1007/978-3-319-01793-8_2

Li, K., Liu, Q., Fang, F., Luo, R., Lu, Q., Zhou, W., Huo, S., Cheng, P., Liu, J., Addy, M., Chen, P., Chen, D., & Ruan, R. (2019). Microalgae-based wastewater treatment for nutrients recovery: A review. In *Bioresource Technology* (Vol. 291, p. 121934). Elsevier Ltd. https://doi.org/10.1016/j.biortech.2019.121934

Li, Min, & Anand, R. K. (2018). Cellular dielectrophoresis coupled with single-cell analysis. In *Analytical and Bioanalytical Chemistry* (Vol. 410, Issue 10, pp. 2499–2515). Springer Verlag. https://doi.org/10.1007/s00216-018-0896-y

Lorenz, M., Malangré, D., Du, F., Baune, M., Thöming, J., & Pesch, G. R. (2020). High-throughput dielectrophoretic filtration of sub-micron and micro particles in macroscopic porous materials. *Analytical and Bioanalytical Chemistry*, *412*(16), 3903–3914. https://doi.org/10.1007/s00216-020-02557-0

Lorrain, P., & Corson, D. R. (1994). Electromagnetic fields and waves. *Choice Reviews Online*, *31*(08), 31-4423-31–4423. https://doi.org/10.5860/choice.31-4423

Maryam Amini, E. M., & Liao, B. (2020). Electrokinetic Membrane Bioreactors. In *Advances in Membrane Technologies: Vol. i* (p. 13). http://dx.doi.org/10.1039/C7RA00172J%0Ahttps://www.intechopen.com/books/advanced-biometric-technologies/liveness-detection-in-biometrics%0Ahttp://dx.doi.org/10.1016/j.colsurfa.2011.12.014

Mata, T. M., Martins, A. A., & Caetano, N. S. (2010). Microalgae for biodiesel production and other applications: A review. *Renewable and Sustainable Energy Reviews*, *14*(1), 217–232. https://doi.org/10.1016/J.RSER.2009.07.020

Medipally, S. R., Yusoff, F. M., Banerjee, S., & Shariff, M. (2015). Microalgae as sustainable renewable energy feedstock for biofuel production. *BioMed Research*

International, *2015*. https://doi.org/10.1155/2015/519513

Melis, A. (2009). Solar energy conversion efficiencies in photosynthesis: Minimizing the chlorophyll antennae to maximize efficiency. *Plant Science*, *177*(4), 272–280. https://doi.org/10.1016/J.PLANTSCI.2009.06.005

Midelet, C., Le Pioufle, B., & Werts, M. H. V. (2019). Brownian Motion and Large Electric Polarizabilities Facilitate Dielectrophoretic Capture of Sub-200 nm Gold Nanoparticles in Water. *ChemPhysChem*, *20*(24), 3354–3365. https://doi.org/10.1002/cphc.201900662

Milledge, J. J., & Heaven, S. (2013). A review of the harvesting of micro-algae for biofuel production. In *Reviews in Environmental Science and Biotechnology* (Vol. 12, Issue 2, pp. 165–178). Springer. https://doi.org/10.1007/s11157-012-9301-z

Molina Grima, E., Belarbi, E. H., Acién Fernández, F. G., Robles Medina, A., & Chisti, Y. (2003). Recovery of microalgal biomass and metabolites: Process options and economics. *Biotechnology Advances*, *20*(7–8), 491–515. https://doi.org/10.1016/S0734-9750(02)00050-2

Molla, S., & Bhattacharjee, S. (2007). Dielectrophoretic levitation in the presence of shear flow: Implications for colloidal fouling of filtration membranes. *Langmuir*, *23*(21), 10618–10627. https://doi.org/10.1021/la701016p

Molla, S. H., & Bhattacharjee, S. (2005). Prevention of colloidal membrane fouling employing dielectrophoretic forces on a parallel electrode array. *Journal of Membrane Science*, *255*(1–2), 187–199. https://doi.org/10.1016/j.memsci.2005.01.034

Mukaibo, H., Wang, T., Perez-Gonzalez, V. H., Getpreecharsawas, J., Wurzer, J., Lapizco-Encinas, B. H., & McGrath, J. L. (2018). Ultrathin nanoporous membranes for insulator-based dielectrophoresis. *Nanotechnology*, *29*(23), 235704. https://doi.org/10.1088/1361-6528/aab5f7

Mustafa, G., Wyns, K., Vandezande, P., Buekenhoudt, A., & Meynen, V. (2014). Novel grafting method efficiently decreases irreversible fouling of ceramic nanofiltration membranes. *Journal of Membrane Science*, *470*, 369–377. https://doi.org/10.1016/j.memsci.2014.07.050

Muylaert, K., Bastiaens, L., Vandamme, D., & Gouveia, L. (2017). Harvesting of microalgae: Overview of process options and their strengths and drawbacks. In *Microalgae-Based Biofuels and Bioproducts: From Feedstock Cultivation to End-Products*. Elsevier Ltd. https://doi.org/10.1016/B978-0-08-101023-5.00005-4

Ozuna-Chacón, S., Lapizco-Encinas, B. H., Rito-Palomares, M., Martínez-Chapa, S. O., & Reyes-Betanzo, C. (2008). Performance characterization of an insulator-based dielectrophoretic microdevice. *Electrophoresis*, *29*(15), 3115–3122. https://doi.org/10.1002/elps.200700865

Papazi, A., Makridis, P., & Divanach, P. (2010). Harvesting Chlorella minutissima using cell coagulants. *Journal of Applied Phycology*, *22*(3), 349–355. https://doi.org/10.1007/s10811-009-9465-2

Pesch, G. R., & Du, F. (2020). A review of dielectrophoretic separation and classification of non-biological particles. *Electrophoresis*, *42*(July), 134–152. https://doi.org/10.1002/elps.202000137

Pesch, G. R., Du, F., Baune, M., & Thöming, J. (2017). Influence of geometry and

material of insulating posts on particle trapping using positive dielectrophoresis. *Journal of Chromatography A*, *1483*, 127–137. https://doi.org/10.1016/j.chroma.2016.12.074

Pesch, G. R., Du, F., Schwientek, U., Gehrmeyer, C., Maurer, A., Thöming, J., & Baune, M. (2014). Recovery of submicron particles using high-throughput dielectrophoretically switchable filtration. *Separation and Purification Technology*, *132*, 728–735. https://doi.org/10.1016/j.seppur.2014.06.028

Pesch, G. R., Kiewidt, L., Du, F., Baune, M., & Thöming, J. (2016). Electrodeless dielectrophoresis: Impact of geometry and material on obstacle polarization. *Electrophoresis*, *37*(2), 291–301. https://doi.org/10.1002/elps.201500313

Pesch, G. R., Lorenz, M., Sachdev, S., Salameh, S., Du, F., Baune, M., Boukany, P. E., & Thöming, J. (2018). Bridging the scales in high-throughput dielectrophoretic (bio-)particle separation in porous media. *Scientific Reports*, *8*(1), 1–12. https://doi.org/10.1038/s41598-018-28735-w

Pethig, R. (2010). Dielectrophoresis: Status of the theory, technology, and applications. *Biomicrofluidics*, *4*(2), 1–35. https://doi.org/10.1063/1.3456626

Pethig, R. (2013). Dielectrophoresis: An assessment of its potential to aid the research and practice of drug discovery and delivery. In *Advanced Drug Delivery Reviews* (Vol. 65, Issues 11–12, pp. 1589–1599). Elsevier. https://doi.org/10.1016/j.addr.2013.09.003

Pethig, R. (2017a). Review—Where Is Dielectrophoresis (DEP) Going? *Journal of The Electrochemical Society*, *164*(5), B3049–B3055. https://doi.org/10.1149/2.0071705jes

Pethig, R. (2017b). How does Dielectrophoresis Differ from Electrophoresis? In *Dielectrophoresis* (pp. 31–48). John Wiley & Sons, Ltd. https://doi.org/10.1002/9781118671443.ch2

Phoochinda, W., & White, D. A. (2003). Removal of algae using froth flotation. *Environmental Technology (United Kingdom)*, *24*(1), 87–96. https://doi.org/10.1080/09593330309385539

Polniak, D. V., Goodrich, E., Hill, N., & Lapizco-Encinas, B. H. (2018). Separating large microscale particles by exploiting charge differences with dielectrophoresis. *Journal of Chromatography A*, *1545*, 84–92. https://doi.org/10.1016/j.chroma.2018.02.051

Pragya, N., Pandey, K. K., & Sahoo, P. K. (2013). A review on harvesting, oil extraction and biofuels production technologies from microalgae. *Renewable and Sustainable Energy Reviews*, *24*, 159–171. https://doi.org/10.1016/J.RSER.2013.03.034

Pulz, O., & Gross, W. (2004). Valuable products from biotechnology of microalgae. *Applied Microbiology and Biotechnology*, *65*(6), 635–648. https://doi.org/10.1007/s00253-004-1647-x

Qari, H., Rehan, M., & Nizami, A. S. (2017). Key Issues in Microalgae Biofuels: A Short Review. *Energy Procedia*, *142*, 898–903. https://doi.org/10.1016/j.egypro.2017.12.144

Qu, X., Alvarez, P. J. J., & Li, Q. (2013). Applications of nanotechnology in water and wastewater treatment. *Water Research*, *47*(12), 3931–3946. https://doi.org/10.1016/j.watres.2012.09.058

Ramos, A., García-Sánchez, P., & Morgan, H. (2016). AC electrokinetics of conducting microparticles: A review. In *Current Opinion in Colloid and Interface Science* (Vol. 24, pp. 79–90). Elsevier. https://doi.org/10.1016/j.cocis.2016.06.018

Ras, M., Lardon, L., Bruno, S., Bernet, N., & Steyer, J. P. (2011). Experimental study on a coupled process of production and anaerobic digestion of Chlorella vulgaris. *Bioresource Technology*, *102*(1), 200–206. https://doi.org/10.1016/j.biortech.2010.06.146

Rashid, N., Rehman, M. S. U., & Han, J. I. (2013). Use of chitosan acid solutions to improve separation efficiency for harvesting of the microalga Chlorella vulgaris. *Chemical Engineering Journal*, *226*, 238–242. https://doi.org/10.1016/j.cej.2013.04.062

Raychaudhuri, S., Dayeh, S. A., Wang, D., & Yu, E. T. (2009). Precise semiconductor nanowire placement through dielectrophoresis. *Nano Letters*, *9*(6), 2260–2266. https://doi.org/10.1021/nl900423g

Ren, Q., & Liang, C. (2020). Insulator-based dielectrophoretic antifouling of nanoporous membrane for high conductive water desalination. *Desalination*, *482*, 114410. https://doi.org/10.1016/j.desal.2020.114410

Ríos, S. D., Salvadó, J., Farriol, X., & Torras, C. (2012). Antifouling microfiltration strategies to harvest microalgae for biofuel. *Bioresource Technology*, *119*, 406–418. https://doi.org/10.1016/j.biortech.2012.05.044

S. Iliescu, F., Sim, W. J., Heidari, H., P. Poenar, D., Miao, J., Taylor, H. K., & Iliescu, C. (2019). Highlighting the uniqueness in dielectrophoretic enrichment of circulating tumor cells. In *Electrophoresis* (Vol. 40, Issue 10, pp. 1457–1477).

Wiley-VCH Verlag. https://doi.org/10.1002/elps.201800446

Saucedo-Espinosa, M. A., & Lapizco-Encinas, B. H. (2015). Design of insulator-based dielectrophoretic devices: Effect of insulator posts characteristics. *Journal of Chromatography A*, *1422*, 325–333. https://doi.org/10.1016/j.chroma.2015.10.030

Schön, J. H. (2015). Electrical Properties. In *Developments in Petroleum Science* (Vol. 65, pp. 301–367). Elsevier. https://doi.org/10.1016/B978-0-08-100404-3.00008-1

Seow, T., Lim, C., Nor, M., Mubarak, M., Lam, C., Yahya, A., & Ibrahim, Z. (2016). Review on Wastewater Treatment Technologies. *International Journal of Applied Environmental Sciences*, *11*(1), 111–126. http://www.ripublication.com

Shi, W., Zhu, L., Chen, Q., Lu, J., Pan, G., Hu, L., & Yi, Q. (2017). Synergy of flocculation and flotation for microalgae harvesting using aluminium electrolysis. *Bioresource Technology*, *233*, 127–133. https://doi.org/10.1016/j.biortech.2017.02.084

Siebman, C., Velev, O. D., & Slaveykova, V. I. (2015). Two-dimensional algal collection and assembly by combining AC-dielectrophoresis with fluorescence detection for contaminant-induced oxidative stress sensing. *Biosensors*, *5*(2), 319–336. https://doi.org/10.3390/bios5020319

Siebman, C., Velev, O. D., & Slaveykova, V. I. (2017). Alternating current-dielectrophoresis collection and chaining of phytoplankton on chip: Comparison of individual species and artificial communities. *Biosensors*, *7*(1). https://doi.org/10.3390/bios7010004

Siebman, C., Velev, O. D., & Slaveykova, V. I. (2018). Probing contaminant-induced alterations in chlorophyll fluorescence by AC-dielectrophoresis-based 2D-algal array. *Biosensors*, *8*(1), 2–13. https://doi.org/10.3390/bios8010015

Singh, G., & Patidar, S. K. (2018). Microalgae harvesting techniques: A review. In *Journal of Environmental Management* (Vol. 217, pp. 499–508). Academic Press. https://doi.org/10.1016/j.jenvman.2018.04.010

Şirin, S., Trobajo, R., Ibanez, C., & Salvadó, J. (2012). Harvesting the microalgae Phaeodactylum tricornutum with polyaluminum chloride, aluminium sulphate, chitosan and alkalinity-induced flocculation. *Journal of Applied Phycology*, *24*(5), 1067–1080. https://doi.org/10.1007/s10811-011-9736-6

Sridharan, S., Zhu, J., Hu, G., & Xuan, X. (2011). Joule heating effects on electroosmotic flow in insulator-based dielectrophoresis. *Electrophoresis*, *32*(17), 2274–2281. https://doi.org/10.1002/elps.201100011

Suehiro, J., Zhou, G., Imamura, M., & Hara, M. (2003). Dielectrophoretic filter for separation and recovery of biological cells in water. *IEEE Transactions on Industry Applications*, *39*(5), 1514–1521. https://doi.org/10.1109/TIA.2003.816535

Suscillon, C., Velev, O. D., & Slaveykova, V. I. (2013). Alternating current-dielectrophoresis driven on-chip collection and chaining of green microalgae in freshwaters. *Biomicrofluidics*, *7*(2). https://doi.org/10.1063/1.4801870

Tang, J., Yang, G., Zhang, Q., Parhat, A., Maynor, B., Liu, D., Din, L. C., & Zhou, O. (2005). Rapid and reproducible fabrication of carbon nanotube AFM probes by dielectrophoresis. *Nano Letters*, *5*(1), 11–14. https://doi.org/10.1021/nl048803y

Teixeira, M. R., & Rosa, M. J. (2006). Comparing dissolved air flotation and conventional sedimentation to remove cyanobacterial cells of Microcystis aeruginosa. Part I: The key operating conditions. *Separation and Purification Technology*, *52*(1), 84–94. https://doi.org/10.1016/j.seppur.2006.03.017

Uduman, N., Bourniquel, V., Danquah, M. K., & Hoadley, A. F. A. (2011). A parametric study of electrocoagulation as a recovery process of marine microalgae for biodiesel production. *Chemical Engineering Journal*, *174*(1), 249–257. https://doi.org/10.1016/j.cej.2011.09.012

Uduman, N., Qi, Y., Danquah, M. K., Forde, G. M., & Hoadley, A. (2010). Dewatering of microalgal cultures: A major bottleneck to algae-based fuels. In *Journal of Renewable and Sustainable Energy* (Vol. 2, Issue 1, p. 012701). American Institute of PhysicsAIP. https://doi.org/10.1063/1.3294480

Vandamme, D., Foubert, I., Fraeye, I., Meesschaert, B., & Muylaert, K. (2012). Flocculation of Chlorella vulgaris induced by high pH: Role of magnesium and calcium and practical implications. *Bioresource Technology*, *105*, 114–119. https://doi.org/10.1016/j.biortech.2011.11.105

Vandamme, D., Pontes, S. C. V., Goiris, K., Foubert, I., Pinoy, L. J. J., & Muylaert, K. (2011). Evaluation of electro-coagulation-flocculation for harvesting marine and freshwater microalgae. *Biotechnology and Bioengineering*, *108*(10), 2320–2329. https://doi.org/10.1002/bit.23199

Vaz, B. da S., Moreira, J. B., Morais, M. G. de, & Costa, J. A. V. (2016). Microalgae as a new source of bioactive compounds in food supplements. *Current Opinion in Food Science*, *7*, 73–77. https://doi.org/10.1016/j.cofs.2015.12.006

Wang, B., Li, Y., Wu, N., & Lan, C. Q. (2008). CO2 bio-mitigation using microalgae.

Applied Microbiology and Biotechnology, *79*(5), 707–718. https://doi.org/10.1007/s00253-008-1518-y

Wang, S., Deng, L., Zheng, D., Wang, L., Zhang, Y., Yang, H., Jiang, Y., & Huang, F. (2018). Control of partial nitrification using pulse aeration for treating digested effluent of swine wastewater. *Bioresource Technology*, *262*, 271–277. https://doi.org/10.1016/j.biortech.2018.04.084

Wang, Y., Du, F., Baune, M., & Thöming, J. (2014). Dielectrophoresis in aqueous suspension: Impact of electrode configuration. *Microfluidics and Nanofluidics*, *17*(3), 499–507. https://doi.org/10.1007/s10404-013-1320-8

Wang, Y., Du, F., Baune, M., & Thöming, J. (2015). Predicting and eliminating Joule heating constraints in large dielectrophoretic IDE separators. *Chemical Engineering Science*, *137*, 235–242. https://doi.org/10.1016/j.ces.2015.06.042

Wang, Yanjuan, Wang, J., Wu, X., Jiang, Z., & Wang, W. (2018). Dielectrophoretic separation of microalgae cells in ballast water in a microfluidic chip. *Electrophoresis*, *40*(6), QQQ. https://doi.org/10.1002/elps.201800302

Wei, M. T., Junio, J., & Ou-Yang, D. H. (2009). Direct measurements of the frequency-dependent dielectrophoresis force. *Biomicrofluidics*, *3*(1). https://doi.org/10.1063/1.3058569

Wei, V., Elektorowicz, M., & Oleszkiewicz, J. A. (2011). Influence of electric current on bacterial viability in wastewater treatment. *Water Research*, *45*(16), 5058–5062. https://doi.org/10.1016/j.watres.2011.07.011

Whitton, R., Ometto, F., Pidou, M., Jarvis, P., Villa, R., & Jefferson, B. (2015). Microalgae for municipal wastewater nutrient remediation: mechanisms, reactors

and outlook for tertiary treatment. In *Environmental Technology Reviews* (Vol. 4, Issue 1, pp. 133–148). Taylor and Francis Ltd. https://doi.org/10.1080/21622515.2015.1105308

Wiley, P. E., Brenneman, K. J., & Jacobson, A. E. (2009). Improved Algal Harvesting Using Suspended Air Flotation. *Water Environment Research*, *81*(7), 702–708. https://doi.org/10.2175/106143009x407474

Wysoczański, T., Sokoła-Wysoczańska, E., Pękala, J., Lochyński, S., Czyż, K., Bodkowski, R., Herbinger, G., Patkowska-Sokoła, B., & Librowski, T. (2016). Omega-3 Fatty Acids and their Role in Central Nervous System - A Review. *Current Medicinal Chemistry*, *23*(8), 816–831. https://doi.org/10.2174/0929867323666160122114439

Xia, L., Li, Y., Huang, R., & Song, S. (2017). Effective harvesting of microalgae by coagulation–flotation. *Royal Society Open Science*, *4*(11). https://doi.org/10.1098/rsos.170867

Yan, Y., Guo, D., & Wen, S. (2017). Joule heating effects on two-phase flows in dielectrophoresis microchips. *Biochip Journal*, *11*(3), 196–205. https://doi.org/10.1007/s13206-017-1209-9

Yang, L. (2012). A Review of Multifunctions of Dielectrophoresis in Biosensors and Biochips for Bacteria Detection. *Analytical Letters*, *45*(2–3), 187–201. https://doi.org/10.1080/00032719.2011.633182

Zhang, H., Chang, H., & Neuzil, P. (2019). DEP-on-a-chip: Dielectrophoresis applied to microfluidic platforms. *Micromachines*, *10*(6), 1–22. https://doi.org/10.3390/mi10060423

Zhao, H. (2011). Double-layer polarization of a non-conducting particle in an alternating current field with applications to dielectrophoresis. *Electrophoresis*, *32*(17), 2232–2244. https://doi.org/10.1002/elps.201100035

Zhao, K., & Li, D. (2018). Tunable Droplet Manipulation and Characterization by ac-DEP. *ACS Applied Materials and Interfaces*, *10*(42), 36572–36581. https://doi.org/10.1021/acsami.8b14430

Zhou, W., Min, M., Hu, B., Ma, X., Liu, Y., Wang, Q., Shi, J., Chen, P., & Ruan, R. (2013). Filamentous fungi assisted bio-flocculation: A novel alternative technique for harvesting heterotrophic and autotrophic microalgal cells. *Separation and Purification Technology*, *107*, 158–165. https://doi.org/10.1016/j.seppur.2013.01.030

Appendix: Additional Figures

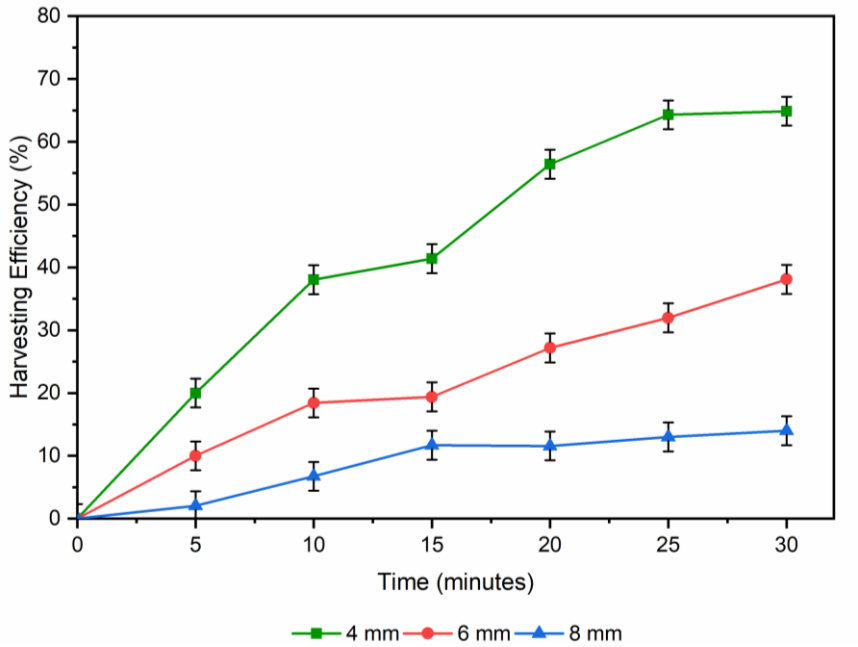

Figure 24. The effect of inter-electrode distance on the harvesting efficiency using 150 V and 250 kHz.

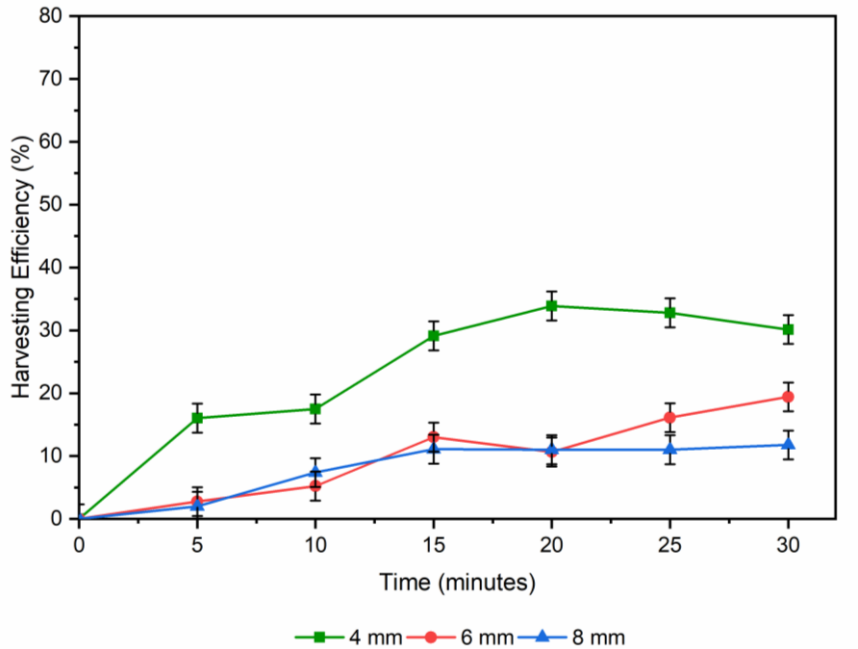

Figure 25. The effect of inter-electrode distance on the harvesting efficiency using 100 V and 250 kHz.